Pharmaceutical Research, Vol. 23, No. 1, January 2006 (© 2006)
DOI: 10.1007/s11095-005-9046-2

Expert Review

Polymer Architecture and Drug Delivery

Li Yan Qiu[1,2] and You Han Bae[1,3]

Received August 12, 2005; accepted October 4, 2005

Abstract. Polymers occupy a major portion of materials used for controlled release formulations and drug-targeting systems because this class of materials presents seemingly endless diversity in topology and chemistry. This is a crucial advantage over other classes of materials to meet the ever-increasing requirements of new designs of drug delivery formulations. The polymer architecture (topology) describes the shape of a single polymer molecule. Every natural, seminatural, and synthetic polymer falls into one of categorized architectures: linear, graft, branched, cross-linked, block, star-shaped, and dendron/dendrimer topology. Although this topic spans a truly broad area in polymer science, this review introduces polymer architectures along with brief synthetic approaches for pharmaceutical scientists who are not familiar with polymer science, summarizes the characteristic properties of each architecture useful for drug delivery applications, and covers recent advances in drug delivery relevant to polymer architecture.

KEY WORDS: drug delivery; nanocarrier; polymer; polymer architecture.

INTRODUCTION

Since the original discovery by Folkman and Long (1) in 1964 that drug molecules, which are hydrophobic and small in size (low molecular weight), diffuse through the wall of silicone tubing at a controlled rate, polymers have occupied a central status in drug release control as well as in the fabrication of drug delivery systems. In comparison with other classes of materials, polymeric materials, including natural, seminatural, and synthetic polymers, present countless opportunities to modulate the properties of drug delivery systems other than to meet several criteria such as biodegradability, biocompatibility, and reproducibility because of their diversity in chemistry, topology, and dimension.

During the past decades, a large number of drug delivery systems, mostly in the forms of microspheres, films, tablets, or implantation devices, have been designed to achieve sustained drug release by taking advantage of the peculiarities of polymers. Today, the concept of "drug delivery" is not limited to prolonging the duration of drug release; instead, it implies at least two strategies for realizing temporal and spatial distribution control in the body. Temporal control stresses the selection of a predetermined kinetics of the drug release during treatment, whereas spatial distribution control aims to precisely direct a drug vehicle to desired sites of activity (2,3). For such controls, significant efforts have been devoted to explore nanotechnology based on the intersection of multiple disciplines of chemistry, biology, and engineering. Nanotechnology focuses not only on formulating therapeutic agents in biocompatible nanocomposites but also on exploiting distinct advantages associated with a reduced dimensional scale within 1–100 nm. Some examples of nanoscaled polymeric carriers involve polymer conjugates, polymeric micelles, and polymersomes (4). Because these systems often exhibit similarity in their size and structure to natural carries such as viruses and serum lipoproteins, they offer multifaceted specific properties in drug delivery applications (5). A viral size minimizes their uptake by the reticuloendothelial system (RES). In addition, the multifunctionality with recognizable moieties and triggered drug release mechanisms can be pursued to further enhance interactions with specific cells and drug concentration in cells. In this way, polymeric systems play a dominant role in drug and gene delivery especially for cancer therapy.

As various nanosystems have been developed, the importance of polymer architecture–property relationships has gradually been realized and emphasized. Polymer architecture describes the shape of a single polymer molecule, which often determines its physicochemical properties. For example, a hydrogel derived from cross-linking random linear copolymers of a temperature-sensitive monomer, *N*-isopropylacrylamide (NIPAAm), and a pH-responsive monomer, methacrylic acid (MAA), has been extensively studied. It has been found that the temperature response disappears with a high-enough content of MAA. On the other hand, the block copolymers with the same composition of NIPAAm and MAA can retain both temperature

[1] Department of Pharmaceutics and Pharmaceutical Chemistry, University of Utah, 421 Wakara Way, Suite 315, Salt Lake City Utah 84108, USA.
[2] College of Pharmaceutical Sciences, Zhejiang University, Hangzhou 310031, China.
[3] To whom correspondence should be addressed. (e-mail: you.bae@m.cc.utah.edu)

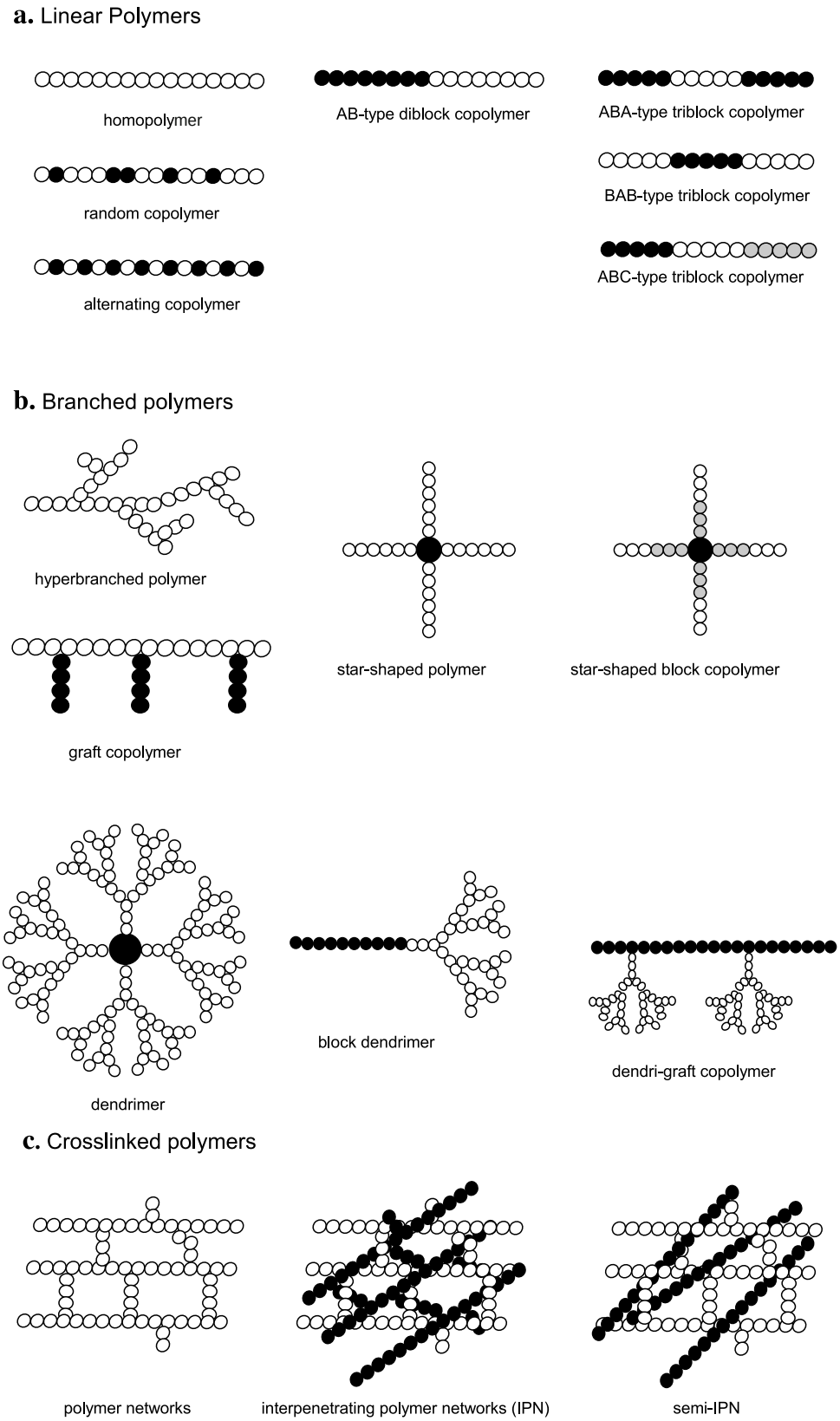

Fig. 1. Polymer architectures: (a) linear polymers, (b) branched polymers, and (c) cross-linked polymers.

Table I. Polymer Architectures and Controlling Factors to Prepare Desired Drug Delivery Outcomes

Architecture	Drug carrier	Property	Controlling factor
Water-soluble linear polymer	Drug conjugate	Solubility	Chain hydrophilicity Solubilizing moiety Drug content
		Biodistribution and cytotoxicity	Molecular weight Electrical charge Targeting groups
		Degradation	Backbone Spacer
		Drug release	Spacer
Block copolymer	Micelle	Shape, critical micelle concentration, and size	Proportion of A block to B block Electrical charge
		Drug encapsulation	Intrinsic affinity between drug and hydrophobic block
		Biodistribution	Molecular weight Proportion of A block to B block Electrical charge Surface hydrophilicity Targeting groups
		Drug release	Interaction between drug and hydrophobic block Conjugation bond between drug and polymer
	Injectable hydrogel (sol–gel transition)	Sol–gel transition temperature and critical gel concentration	Molecular weight Proportion of A block to B block
	Polymersome	Shape	Proportion of A block to B block
		Membrane thickness	Length of hydrophobic chain
Hyperbranched polymer	Micelle	Shape, critical micelle concentration, and size	Proportion of hydrophilic domain to hydrophobic domain Electrical charge Complexed Drug content
		Cytotoxicity and gene transfection efficiency	Molecular weight Electrical charge Surface hydrophilicity
Graft polymer	Injectable hydrogel (sol–gel transition)	Lower critical solution temperature	Graft ratio Molecular weight
	Micelle	Critical micelle concentration	Graft ratio
Star polymer	Unimolecular micelle	Drug encapsulation	Dimension of hydrophobic core Arm number
	Injectable hydrogel (sol–gel transition)	Lower critical solution temperature and gel strength	Arm number
Dendrimer	Unimolecular micelle	Size, drug-loading capability, and efficiency	Generation number Electrical charge

and pH responsiveness, which is attributed to the microphase separation of different units (6). This exemplifies the significance of architecture and monomer sequence in manipulating polymer properties. Any polymer selected for drug delivery formulation is commonly classified according to chemical nature [such as polyester, polyanhydride, poly (amino acid)], backbone stability (biodegradable, nonbiodegradable), and water solubility (hydrophobic, hydrophilic) (7). The polymer architecture as well as its related syntheses and characterization, however, is relatively unfamiliar to pharmacists. Thus, this review is organized on the basis of polymer architecture and highlights its effect on drug delivery.

Polymer architectures relevant to drug delivery applications are presented in Fig. 1. Linear polymers especially refer to water-soluble polymers to create polymer–drug conjugates. Block copolymers used in building supramolecular structures are linear but are classified as different architectures. Branched copolymers are characterized by the presence of branch points and more than two end groups, which comprise a class of polymers somewhere between linear polymers and polymer networks. Numerous studies have

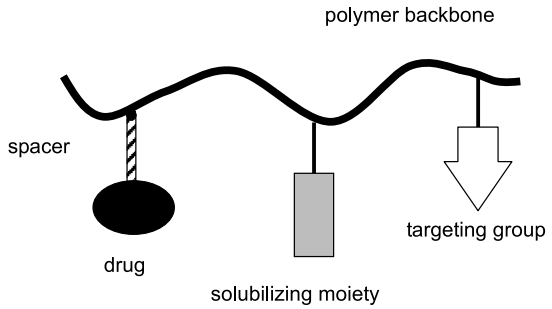

Fig. 2. Ringsdorf model of polymer–drug conjugate consisted of five main elements: polymeric backbone, drug, spacer, targeting group, and solubilizing moiety.

revealed that branched polymers offer significantly different physical properties from linear polymers and polymer networks, such as melt rheology, mechanical behavior, and solution properties (8). Although undesirable branching occurs in many polymerization reactions, here, branched polymers only refer to those with branches prepared via controlled polymerization techniques, including hyperbranched, graft, star-shaped polymers and dendron/dendrimers. Because the majority of cross-linked polymers, including interpenetrating polymer networks (IPN) or semi-IPN, involve chemical cross-linking techniques to form drug delivery systems beyond nanoscale in size, they will not be covered in this summary. Table I presents a brief summary of polymer architectures and controlling factors attributing to nanosized drug carrier properties.

LINEAR WATER-SOLUBLE HOMOPOLYMERS OR COPOLYMERS

Linear polymers own the simplest architectural form. Their two potential advantages connected to nanotechnology have been specially noted. One is the formation of random-coil structures of 5–15 nm in size in good solvents depending on molecular weight and polymer–solvent interactions; the other is the ability of tailored multivalency by introducing functional comonomers along the polymer backbone. Typical applications of linear water-soluble polymers center on polymer–drug conjugations.

Linking drugs onto polymers for drug-targeting purpose was first reported in the 1950s. A general model for polymer–drug conjugation was proposed by Ringsdorf (9) in 1975, which was based on the combination of chemistry and biology and consisted of five main elements: polymeric backbone, drug, spacer, targeting group, and solubilizing moiety (Fig. 2). The most important aspect of this model lies in the localization of the conjugates in target subcellular compartments via cell-specific or nonspecific uptake mechanisms. To date, almost all polymer–drug conjugates have been derived from this symbolic model. This development has promoted the rational selection of individual elements within this model for improved drug efficiency in the body. Now, more than ten polymer–drug conjugates have entered phase I/II clinical trials, not only proving the value of linear polymers as drug carriers but also encouraging further research and translation from laboratory to clinical practice (10).

Polymer Main Chain

A representative list of polymers frequently used for carrying antitumor agents or other drugs includes vinyl polymers, polysaccharides, poly(amino acids), proteins, and poly (ethylene glycol) (PEG). A number of reviews have addressed the application of water-soluble polymers as drug carriers (7,11).

Considering radical polymerization mechanisms and numerous options in chemical structure, vinyl polymers can be tailor-made to acquire required properties for drug delivery. At present, significant studies have focused on *N*-(2-hydroxypropyl methacrylamide) (HPMA) copolymers (12,13). The first polymer conjugate entered phase I clinical trials as PK1 (FCE28068; Scheme 1) in 1994, which utilized an HPMA copolymer as a carrier for the anticancer agent doxorubicin. Later, PK1 reached phase II clinical trials for

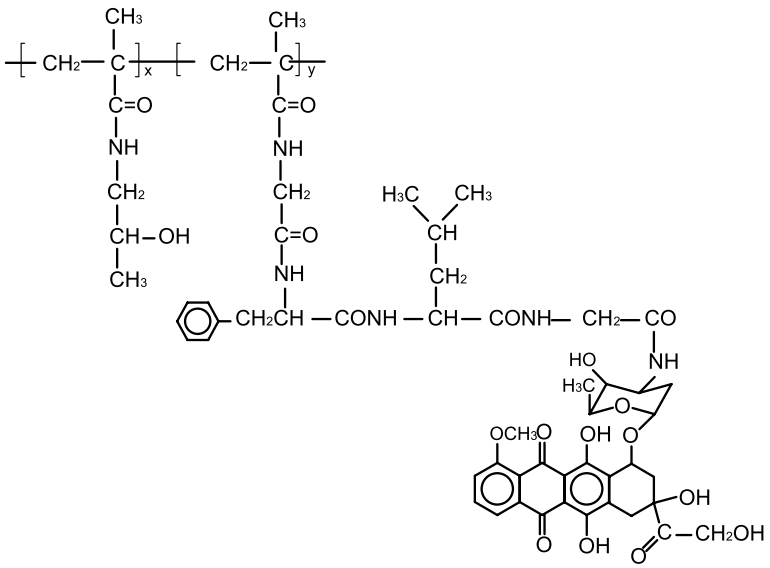

Scheme 1. Poly(*N*-(2-hydroxypropyl methacrylamide)) copolymer containing doxorubicin PK1 (FCE28068).

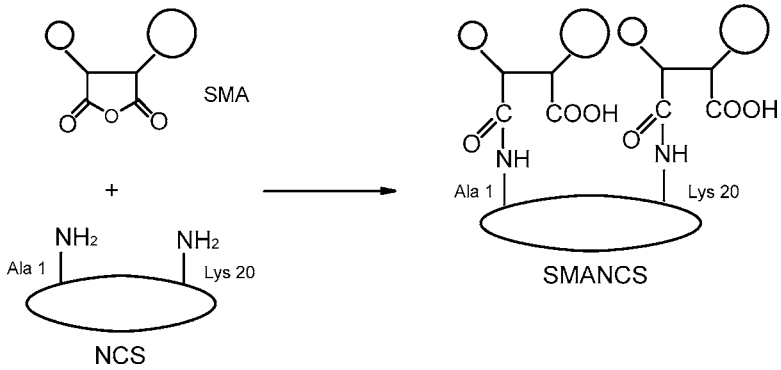

Scheme 2. Neocarcinostatin-conjugated poly(styrene-*co*-maleic acid/anhydride) (SMANCS).

the treatment of breast, colon, and nonsmall-cell lung cancers. Biodistribution, immunogenicity, and biological activity studies have proven that polyHPMA (or PHPMA) is nontoxic and nonimmunogenic *in vivo*. Poly(styrene-*co*-maleic acid/anhydride) (SMA) is another proven vinyl polymer in drug delivery. Its conjugation (SMANCS; Scheme 2) with the antitumor protein neocarcinostatin (NCS) has already been marketed in Japan to treat primary hepatoma and secondary tumor of the liver (14). Poly(*N*-vinylpyrrolidone) (PVP), with an active group on one chain end introduced by a chain transfer agent during polymerization, can conjugate with certain drugs (e.g., *para*-nitroaniline and interleukin-6) to increase drug solubility and stability (15–17). A noteworthy example of this kind of polymer is poly(vinylpyrrolidone-*co*-dimethyl maleic anhydride) (PVD; Scheme 3a) synthesized by Kishida (18). *In vivo* tests indicated that it was specifically taken up by renal proximal tubular epithelial cells, resulting in selective delivery of the drug to the kidney. Poly(amino acids), such as poly(L-lysine), poly(L-glutamic acid), and poly[(*N*-hydroxyalkyl) glutamine] (Scheme 4), can be obtained by ring-opening polymerization of the *N*-carboxy anhydride monomers (19,20). The functional side groups of these polymers offer the possibility of coupling with drug molecules. Proteins like serum albumin have been used to prepare conjugates (21). The major disadvantage of these molecules is their complicated chemical compositions, which make it difficult to characterize the products. As for polysaccharides, much attention has been directed toward dextran, alginate, and chitosan/chitin derivatives (22–24). These natural polymers have good biocompatibility and contain functional side groups ready for drug conjugation and/or modification. Their intrinsic chemical structure and biodegradability offer some convenience to design drug conjugates. PEG has most often been used to modify a number of therapeutic proteins by enhancing their stability, plasma half-life, and reducing their immunogenicity *in vivo*. Besides, PEG has proven to improve the therapeutic index of anticancer agents in a conjugate form (25,26). Recently, a water-soluble polyacetal bearing amino-pendant groups (APEG) for drug linkage (Scheme 5) was synthesized by terpolymerization of PEG, divinyl ethers, and serinol (27). Because this polyacetal displays pH-dependent degradation with a faster hydrolysis rate at acidic pH and is not inherently hepatotropic after intravenous injection, it has the potential to be developed as biodegradable carriers for tumor targeting of anticancer agents.

During the development of various polymer carriers, it was revealed that the molecular weight (MW), polydispersity, charge, and the hydrophilic–hydrophobic character of the polymer main chain impact drug biodistribution, clearance, biological activity, and toxicity to a great extent. The ability of a polymer to prolong the circulating duration (decreased

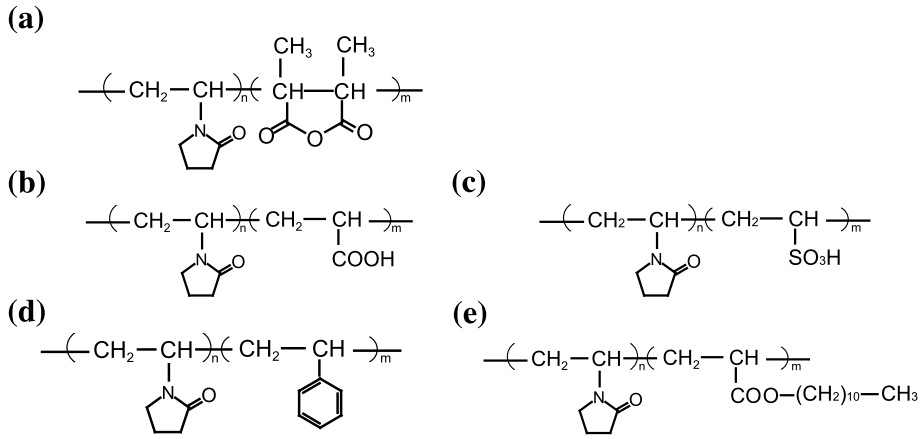

Scheme 3. (a) Poly(vinylpyrrolidone-*co*-dimethyl maleic anhydride); (b) poly(vinylpyrrolidone-*co*-acrylic acid); (c) poly(vinylpyrrolidone-*co*-vinylsulfonic acid); (d) poly(vinylpyrrolidone-*co*-styrene); and (e) poly(vinylpyrrolidone-*co*-vinyl laurate).

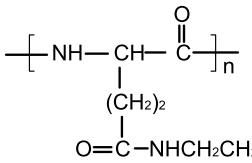

Scheme 4. Poly[(*N*-hydroxyalkyl) glutamine].

clearance rate) is the prerequisite to insure that a drug carrier reaches and accumulates at its target sites by utilizing characteristics of tumor tissues such as leaky vasculature with increased permeability and poor lymphatic draining. This leads to preferential extravasation and subsequent retention of high molecular weight conjugates in the solid tumor, which is known as the enhanced permeability and retention (EPR) effect. The rationale of delivering a drug in polymer conjugate form stems from the fact that an increase in molecular weight significantly alters the biodistribution of the conjugates, thus achieving passive targeting in a particular tissue. As the molecular weight of a water-soluble polymer increases, there is greater enhancement in circulation times and better accumulation in tumor tissue by EPR (28). On the other hand, because ~45 kDa molecular weight was demarcated as the limit for renal filtration, the molecular weight of inert polymers generally should not exceed this limit; otherwise, they will accumulate in the body. However, this limit has not been stressed for biodegradable polymers (29).

Riebeseel *et al.* (30) investigated PEG MW-dependent cytotoxicity of PEG-methotrexate (PEG-MTX). *In vitro* cytotoxicity evaluation with two adherents and three suspensions of human tumor cell lines revealed that IC_{50} values increased with the size of the drug–polymer conjugates [IC_{50} for PEG-MTX_{750}, PEG-MTX_{2000}, and PEG-MTX_{5000} (the number is the MW of PEG): ~0.6–3 μM; for PEG-$MTX_{10,000}$ and PEG-$MTX_{20,000}$: ~2–7 μM; and for PEG-$MTX_{40,000}$: >6 μM]. This result was attributed to the reduced rate of cellular uptake for conjugates with a higher MW. In contrast to the *in vitro* results, PEG-$MTX_{40,000}$ exhibited the highest *in vivo* antitumor activity. At a dose of 20 mg/kg, PEG-$MTX_{40,000}$ showed superior efficacy compared with free MTX at its optimal dose (100 mg/kg), whereas PEG-MTX_{5000} (at 40 and 80 mg/kg) and PEG-$MTX_{20,000}$ (at 20 and 40 mg/kg) were either significantly or slightly less active than free MTX. Herein, the prolonged circulation time and EPR effect of high MW explain the increased targeting actions of the polymer–drug conjugates on solid tumors. Similarly, in the case of PEG–doxorubicin (Dox) conjugates, the conjugate containing the highest MW of PEG revealed to have the longest plasma residence time and consequently the greatest tumor accumulation (Fig. 3) (31). When comparing *in vivo* pharmacokinetics of polyacetal (MW 86,000 g/mol, higher than the renal threshold)–Dox with PHPMA (MW 30,000 g/mol)–Dox, plasma levels of the former were significantly higher than that of the latter after 5, 48, and 72 h, and polyacetal–Dox displayed elevated tumor accumulation levels at 48 and 72 h (Fig. 4) (27).

As for PVD, it was found that molecular size between 6 and 8 kDa showed the highest renal accumulation compared to either a lower molecular weight of 3 kDa or a higher molecular weight of 14 kDa, which resulted from two paradoxical effects of increasing molecular weight: extended blood residence and increased difficulty in entering the specific tissue (32). When PVD–superoxide dismutase conjugates with different drug contents were examined, it was also observed that the specific bioactivity of the conjugates gradually decreased with increasing degrees of drug modification (increase in MW). Thus, selecting the proper molecular weight for a given linear polymer is of primary importance in controlling special distribution *in vivo*.

Chemical structure and electrical charge also influence the biodistribution of polymer–drug conjugates. PVP showed the longest mean resident time after an i.v. injection among various polymers with similar molecular weights, e.g., polyacrylamide (PAAm), poly(dimethyl acrylamide) (PDAAm), poly(vinyl alcohol) (PVA), and dextran. Its tissue distribution was extremely restricted (17). The elimination rate of anionic PVP derivatives from the blood increased as the number of anionic groups increased. PVP was effectively retained in the blood and gradually excreted into the urine instead of concentrating in the kidneys. The clearance of carboxylated PVP [poly(vinylpyrrolidone-*co*-acrylic acid); Scheme 3b] and sulfonated PVP [poly(vinylpyrrolidone-*co*-vinylsulfonic acid); Scheme 3c] from the blood was almost similar (Fig. 5a). However, carboxylated PVP efficiently accumulated in the kidney, whereas sulfonated PVP was rapidly excreted in the urine. Renal levels of carboxylated PVP were about fivefold higher than sulfonated PVP (Fig. 5b) (33).

Solubility is another factor that needs to be taken into consideration. A soluble polymer is used to vastly improve the solubility of hydrophobic drug, but, in turn, the solubility of the polymer itself would decrease. Therefore, the quantity of drug in a conjugate should be optimized. The study on hydrophobic PVP derivatives reflected the influence of polymer solubility on biodistribution (34). Poly(vinylpyrrolidone-*co*-styrene) [poly(VP-*co*-St); Scheme 3d] and poly(vinylpyrrolidone-*co*-vinyl laurate) [poly(VP-*co*-VL); Scheme 3e] were synthesized by radical copolymerization. Poly(VP-*co*-St) efficiently accumulated in the spleen, whereas poly (VP-*co*-VL) accumulated in the liver. Their pharmacokinetics was quite different from that of PVP.

Drug and Spacer

In polymer–drug conjugates, the drug can be included either as a unit within polymer backbone or as a part of

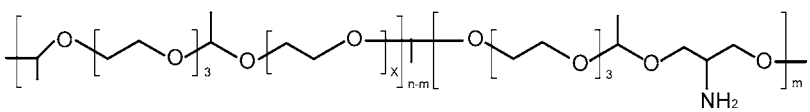

Scheme 5. Structure of polyacetal (APEG) synthesized by terpolymerization of PEG, divinyl ethers, and serinol.

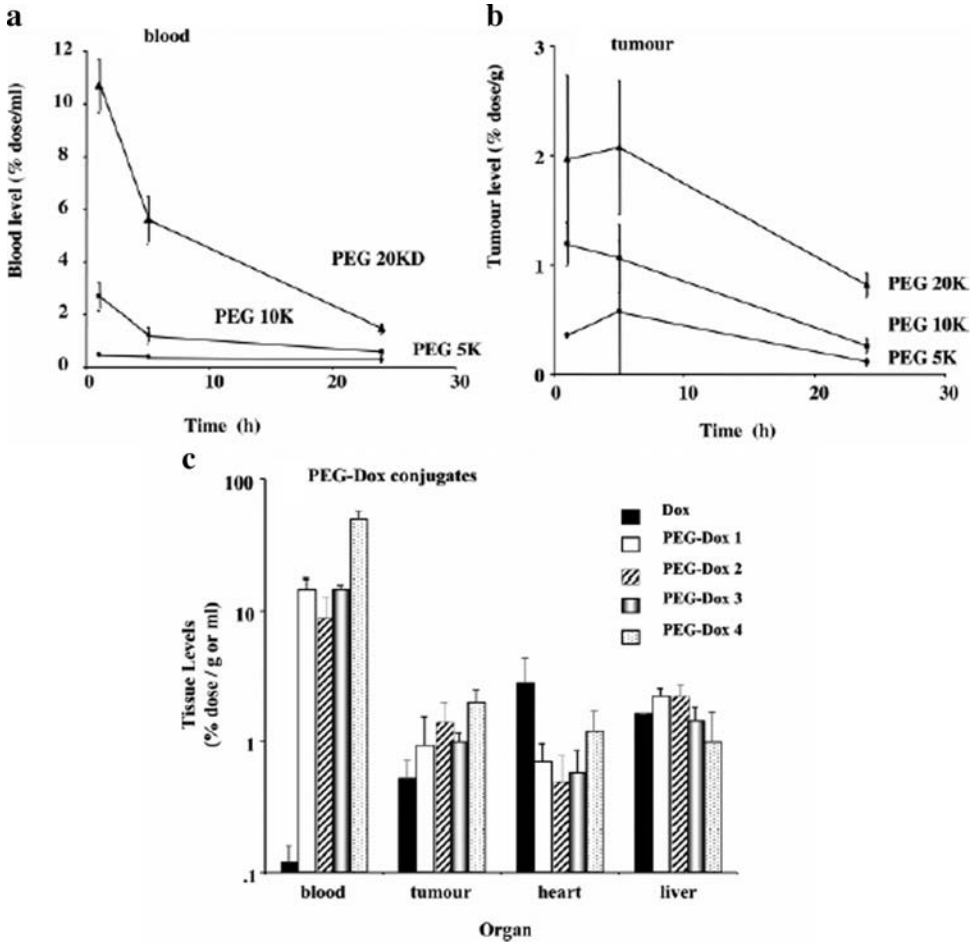

Fig. 3. Biodistribution of ^{125}I-labeled poly(ethylene glycol)s (PEGs) and PEG–doxorubicin (Dox) conjugates at 1 h after i.v. administration to mice bearing sc B16F10 tumors. (a) The time course of radioactivity detected in blood of ^{125}I-labeled PEGs; (b) the time course of radioactivity detected in tumor tissue of ^{125}I-labeled PEGs; (c) the total Dox recovered in various tissues of PEG–Dox conjugates: PEG–Dox1 (PEG 5K, Dox content 3.0–7.4 wt.%), PEG–Dox 2 (PEG 10K, Dox content 5.0 wt.%), PEG–Dox3 (PEG 10K, Dox content 4.3 wt.%), PEG–Dox4 (PEG 20K, Dox content 2.7 wt.%) (31).

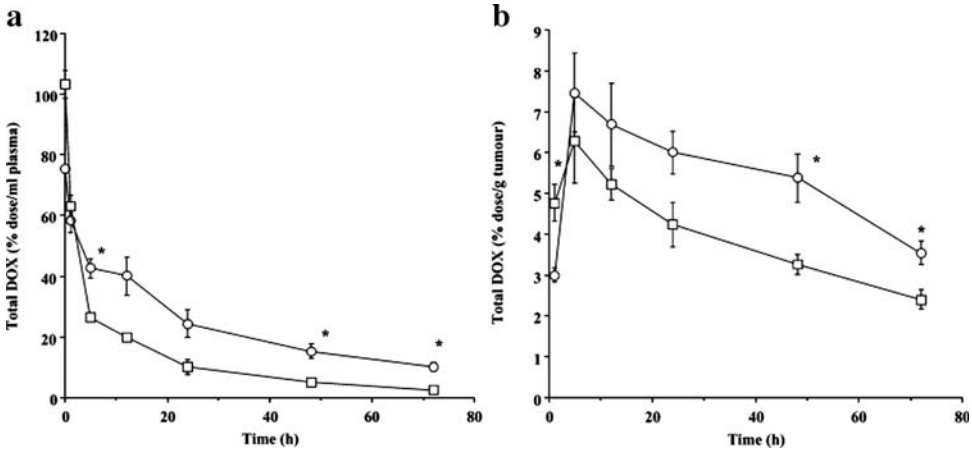

Fig. 4. The distribution of amino-pendant group (APEG)–Dox (○) and, for comparison, *N*-(2-hydroxypropyl methacrylamide) (HPMA) copolymer–Dox (□) administered i.v. (5 mg/kg Dox equivalent) to mice bearing sc B16F10 melanoma tumors. (a) Plasma and (b) tumor (* indicated statistical significance $p < 0.05$) (27).

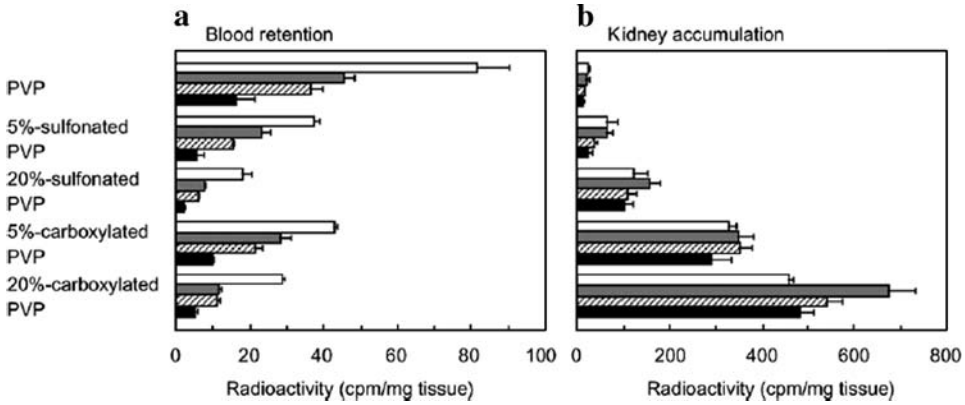

Fig. 5. (a) Blood retention and (b) kidney accumulation of poly(*N*-vinylpyrrolidone) (PVP) and anionized PVP derivatives after i.v. injection in mice. Mice were intravenously injected with ^{125}I-labeled polymers. The radioactivity was measured by a γ-counter. Each value is the mean ± SD (n = 5). □: 1 h, ▨: 3 h, ▨: 6 h, ■: 24 h after i.v. injection (33).

pendant groups. To facilitate the release or reaction of a drug at a specific site, the majority of conjugates bear drugs as side groups. If the polymer possesses multiple active groups for linkage, the resulting conjugate can contain multiunits of a drug, such as HPMA copolymer, poly(amino acid), and polysaccharides. For vinyl polymers, there are two methods to prepare polymer–drug conjugates. One method is copolymerization of a monomer, a monomer drug, and/or monomer-targeting ligand. Radical polymerization requires careful optimization processes to insure adequate control of the molecular weight, molecular weight distribution, and drug incorporation (composition). The other method, known as polymer analogous reaction (conjugation of drug molecules to an existing polymer backbone), has been applied more frequently. The conjugation reaction is relatively uniform in terms of reactivity. In some cases, presynthesizing peptidyl prodrugs (or drug-peptidyl spacer) becomes the preferred route, for this can insure the conjugation of well-characterized drug derivatives to polymers with shorter side chains. By using this method, it is also easier to control the drug content in the resultant conjugate by modulating the feed ratio of polymer and drug (12).

The drug can be linked either directly or via a spacer group to the polymer backbone. If a drug regains its pharmacological activity only after its release from the conjugate, the conjugates are termed macromolecular prodrugs. Polymer–drug conjugates that retain the activity as a whole can be regarded as polymer drugs (35). Following congregation at a specific site because of the EPR effect, polymer–drug conjugates will be internalized into cells through endocytotic pathways with or without the assistance of targeting moieties. Endocytotic internalization involves membrane invagination with concomitant capture of macromolecules, which are then transferred into the early endosomal compartment and later into a secondary lysosomal compartment, via a series of vesicle fusion events. Like the plasma membrane, the lysosomal membrane is a natural barrier to macromolecular transfer and thus only allows low molecular weight products to escape into the cytoplasm. Ideally, macromolecular conjugates should be stable and pharmacologically inactive while circulating in the blood stream, but release the drug from the polymeric conjugate after uptake into the cells. Most of the drug release from polymer backbone is warranted through the controlled hydrolysis of a spacer group. According to the different hydrolysis mechanism, spacers can be designed to respond to the passive hydrolysis, acid catalytic hydrolysis, and enzymatic hydrolysis, reviewed in detail by Soyez *et al.* (35).

Chemical bonds comprised of ester, carbonate, amide, and urethane readily hydrolyze. The hydrolysis rate decreases in order from ester to carbonate to urethane to amide. Any drug combined into the polymer backbone or linked to the spacer through such a bond will be released in an aqueous environment. Hydrolysis without obvious cell specificity is their main shortcoming.

More than 40 enzymes in the lysosomes have been identified with the ability to break down almost all biologically important materials. Peptidyl spacers play an important role in facilitating intracellular enzymatic degradation. Furthermore, it has been emphasized that the structure of peptidyl spacers directly affects the drug release rate from the polymer. The following general conclusions have been drawn for enzyme-sensitive polymer–drug conjugates used for tumor cell targeting: (1) a tripeptide is the shortest substrate for enzymatic cleavage; (2) the cleavage rate increases with increasing spacer length for a similar amino acid sequence; (3) the terminal moiety markedly alters the rate of drug release; and (4) the type of drug and polymer backbone will influence the enzymatic hydrolysis rate (36,37). As an interesting example, a spacer containing an aromatic

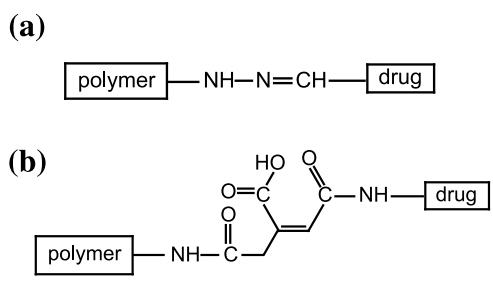

Scheme 6. (a) Hydrazone and (b) *N-cis*-aconityl spacer.

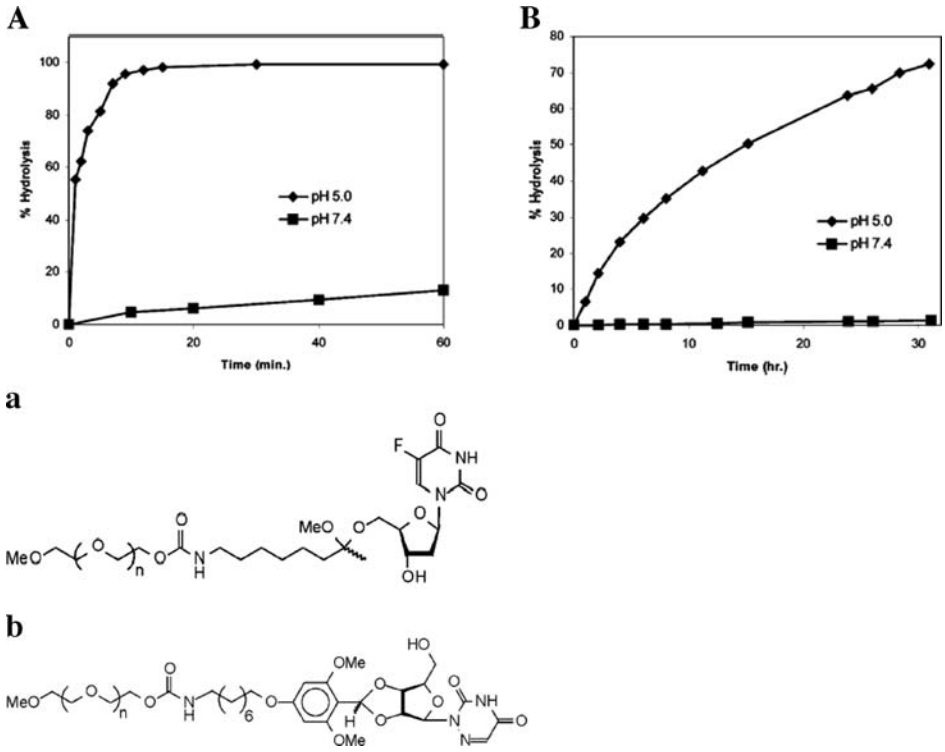

Fig. 6. (A) Hydrolysis rate of (a) 5-fluoro-2′-deoxyuridine-poly(ethylene oxide) (PEO) acetal conjugate at pH 5.0 and 7.4; and (B) hydrolysis rate of conjugate (b) 5-fluorouridine-PEO acetal conjugate at pH 5.0 and 7.4 (42).

azo bond has been used to link a drug to a polymer, achieving colon-specific drug delivery by taking advantage of its sensitivity to large intestinal azoreductase.

Polymers entering the endosomal or lysosomal compartment are exposed to an acid environment. The pH drops from physiological 7.4 to 5–6 in endosomes and 4–5 in lysosomes (38). Using pH-sensitive spacers in polymer–drug conjugates is relatively simple and economic. Shen and Ryser (39) were the first to describe the linkage of daunomycin to aminoethyl polyacrylamide beads or poly(D-lysine) through the pH-sensitive spacer *N-cis*-aconityl or *N*-maleyl and proved the pH-dependent hydrolysis. So far, hydrazones and *N-cis*-aconityl (Scheme 6) have been used most frequently for preparing polymer–drug conjugates (40,41). Less attention has been paid to spacers containing substituted trityl, acetal, or imino groups. These kinds of spacers have been in-depth reviewed by Ulbrich and Šubr (38). Recently, acetals were investigated for their potential as acid-accelerating hydrolysis linkages in polymer–drug conjugations (Fig. 6) (42). Acetals can be prepared using a variety of hydroxy groups, and the hydrolysis rate can be tuned according to the chemical structure. Polyacetal was reported as an interesting polymer for releasing drugs in specific cells through pH-sensitive hydrolysis of the backbone rather than the spacer (27,43).

Targeting Groups

Prolonged plasma circulation is the driving force for increased tumor targeting. Active targeting with tumor-specific agents promotes the internalization of the carriers into the cells. Thus, several reviews have expatiated a broad spectrum of targeting moieties proposed as candidates for tissue- or tumor-selective targeting: hormones, carbohydrates, antibodies, antibody fragments, and epitopes (28,44,45); however, the details of this area are beyond the scope of this review summary.

BLOCK COPOLYMERS

Block copolymers are defined as polymers that have two or more blocks or segments arranging in the main chain and can be classified according to their architecture as AB-type diblock, ABA- or BAB-type triblock, and multiblock, where A represents the soluble block in a selected solvent and B designates the insoluble block (46). Because of the intrinsic affinity interactions of those segments with the same physicochemical properties, block copolymers often show a tendency to form self-assemblies in solvents. However, block mobility is quite restricted for steric reasons, and the self-assembled domains composed of identical blocks consequently fall into nano- or microsized scale and are segregated into the most entropically stabilized state. The detailed features of self-assembled domains are sensitive to the architecture of the block copolymer. It is practical to tune the physicochemical properties of the polymer to endow new functionalities of either the core or the surface of such a self-assembly.

Among block copolymers, linear amphiphilic block copolymers play an essential role in carrying drugs on a nanoscale level (47). Amphiphilic block polymers specifically refer to those having both hydrophilic (water) and hydro-

phobic (oil) blocks in the same polymer chain, which can then build spherical polymeric assemblies in aqueous solution, called "polymeric micelles", with nanosized and core-shell segregated domains. Studies on polymeric micelles were initiated in 1960s. But the first attempt to utilize block copolymer micelles as drug carriers was not reported until 1984 by Bader *et al.* (48) and Pratten *et al.* (49). Although their study was limited to *in vitro* tests, they suggested that the polymeric micelle would act as a drug carrier similar to natural lipoproteins. A drug was conjugated to one segment of the block polymer to form the core, and the other segment PEG remained unmodified as a water-soluble shell. Kabanov *et al.* (50) reported the enhancement of drug efficacy when a neuroleptic drug was associated with a micelle composed of polymeric amphiphile poly(ethylene oxide)$_{26}$–poly(propylene oxide)$_{40}$–poly(ethylene oxide)$_{26}$ (PEO–*b*-PPO–*b*-PEO) known as Pluronic P-85. In the late 1980s, Kataoka's group (51–53) initiated their work on drug-conjugated micelles, utilizing the condensation reaction between the glycosidic primary amino group of Dox and the carboxylic groups from the anionic block copolymer poly(ethylene glycol)–*b*-poly(α,β-aspartic acid) (PEG–*b*-Pasp; Scheme 7). Following the animal experimentation, this micelle system is now undergoing phase II testing. Since the 1990s, a significant increase in the publication on this topic can be noticed. At present, micelles formed by various amphiphilic block copolymers are being developed for delivering anticancer, anti-inflammatory, antiviral, antibacterial, imaging agents and DNA. Overall, block copolymer-based drug delivery systems have been successfully used to (1) target drugs to specific physiological sites (organs, tissues, or cells), (2) solubilize hydrophobic drugs, (3) increase drug stability, and (4) control drug release, realizing the efficiency maximum and toxicity minimum of drug (54).

In the past three decades, a large number of known polymerization techniques, including radical, anionic, cationic, photo, group transfer, and Ziegler/Natta polymerizations, have been tried to obtain amphiphilic block copolymers, which have been reviewed by Kumar *et al.* (46). Using conventional radical polymerization, a block copolymer with narrow molecular weight distribution is rarely produced because of the termination modes (recombination and disproportionation) and the presence of side reactions such as chain transfer (54). To overcome this problem, living polymerization has become the most widely used technique. Furthermore, this method provides additional advantages in that the molecular weight of the individual blocks (variation of initiator/monomer ratio), the volume ratio (variation of monomer/monomer ratio), as well as the block arrangement (AB-, ABA-, and BAB-type) can be adjusted to create the structure desired. Generally, this technique is carried out by sequentially adding monomers to obtain AB, ABC, and ABA using a monofunctional initiating system or to obtain BAB and CBABC architectures using a bifunctional initiator

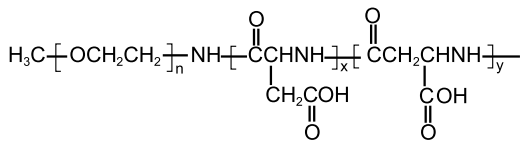

Scheme 7. Poly(ethylene glycol)-*b*-poly(α,β-aspartic acid).

system. Adding different monomer at the same time is applicable when the reactivity of the monomers is very different and permits a mono- and bifunctional initiation, which means that the block propagation of second monomer does not begin until the polymerization of the more reactive first monomer is complete (55). Coupling terminal functionalized blocks is an alternative method in practice to synthesize AB and ABA block polymers. However, a successful synthesis depends on the following requirements: no side reactions occur; 100% end-group functionality of copolymers is necessary for a complete coupling reaction; and the functional end groups of different blocks must be in the exact mole ratio.

Types of Polymeric Micelle

To date, the three major types of micelle delivery systems based on linear block copolymers are (1) common block copolymer micelle, (2) drug-conjugated block copolymer micelle, and (3) block ionomer complex micelle (Fig. 7).

PEG is most often used as a hydrophilic segment because of its flexibility, nontoxicity, and hydrophilicity. However, the options available for the hydrophobic block are much broader. For example, the AB-type block polymer PEG–*b*-polyester, such as PEG–*b*-poly(D,L-lactide) (PDLLA), PEG–*b*-poly(lactide-*co*-glycolide) (PLGA), and PEG–*b*-poly(ε-caprolactone) (PCL), is a popular family of block polymers used for drug delivery (56). PEO–*b*-poly(γ-benzyl-L-glutamate) was developed later (57). Two long-chain fatty acyl groups in phospholipids are hydrophobic, and they have been used successfully as the hydrophobic core-forming group. By changing the hydrophilic segments, a series of lipid derivatives have been reported for preparing drug-loaded micelles including PEG–phosphatidyl ethanolamine (PE), poly(2-alkyl-2-oxazoline)–PE, poly(acryloyl morpholine)–PE, PVP–PE, and polyglycerol–phosphatidylglycerol (Scheme 8) (58–60). Recently, Chang *et al.* (61,62) reported several kinds of amphiphilic diblock copolymers composed of PEG and hydrophobic poly[bis(ethyl glycinat-*N*-yl) phosphazene] or poly[bis(trifluoroethoxy) phosphazene] (Scheme 9a), which were synthesized via controlled cation-induced polymerization of a phosphoranimine at an ambient temperature using a PEG–phosphoranimine macroinitiator. In a similar method, using methoxyethoxyethoxyl group (MEEP) as hydrophilic block, amphiphilic diblock polystyrene–*b*-poly-[bis(methoxyethoxyethoxy) phosphazene] (PS–*b*-PMEEP; Scheme 9b) and MEEP-phenyl/MEEP copolyphosphazene (Scheme 9c) were synthesized and characterized (63,64).

Drug-conjugated block copolymer micelles are developed by taking advantage of the interaction between a drug and one segment of the soluble block copolymer on various mechanisms to build the hydrophobic polymer–drug core of micelle. For example, cationic PEG–*b*-poly(L-lysine) (PLL), PEG–*b*-poly(dimethylaminoethyl methacrylate) (DMAEMA), and PEG–*b*-linear polyethyleneimine (PEI) combine with DNA through electrostatic interaction to form potential nonviral vectors for gene therapy (65–67). PEG–*b*-Pasp or PEG–*b*-poly(L-glutamic acid) with carboxylates facilitate to introduce *cis*-diamine dichloroplatinum (II) (CDDP) into a stable micelle core via chelation effect

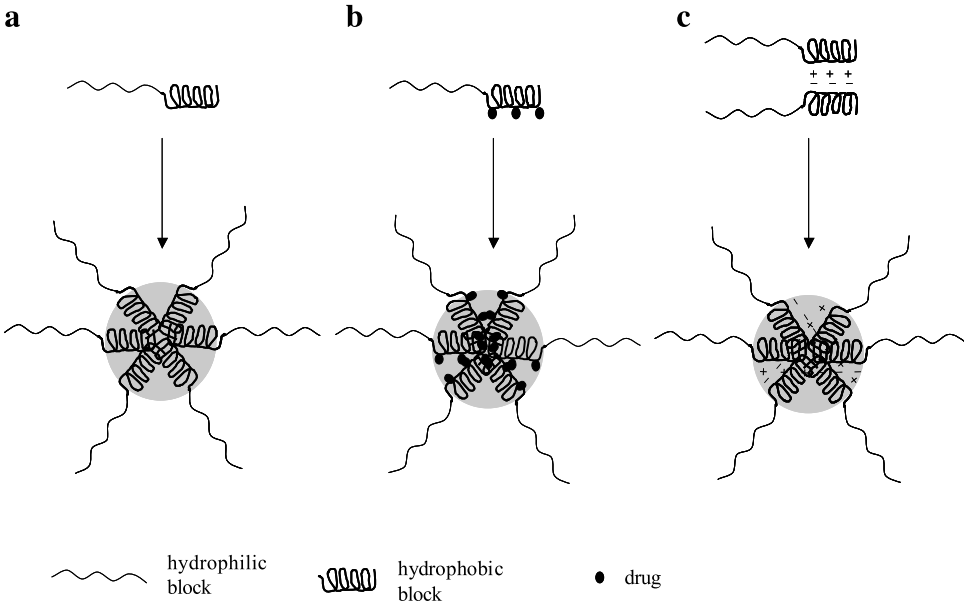

Fig. 7. Three major types of micelles based on linear block copolymer: (a) common block copolymer micelle, (b) drug-conjugated block copolymer micelle, and (c) block ionomer complex micelle.

(68,69). Likewise, the imaging diagnostic moiety, iodine, was loaded into a micelle by the specific chemical modification between tridodobenzoic acid *N*-hydroxysuccinimide ester and PLL block of PEO–*b*-PLL. X-ray computed tomography investigation has demonstrated its efficacy *in vivo*, suggesting a good method to circumvent the serious problems arising from the rapid disappearance of low-molecular weight contrast agents (70).

Polyion complex (PIC) micelles are comprised of two block copolymers with opposite charges. The formation of PIC micelles was first proposed by Harada and Kataoka (71) for the pair of PEG–*b*-PLL and PEG–*b*-Pasp block copoly-

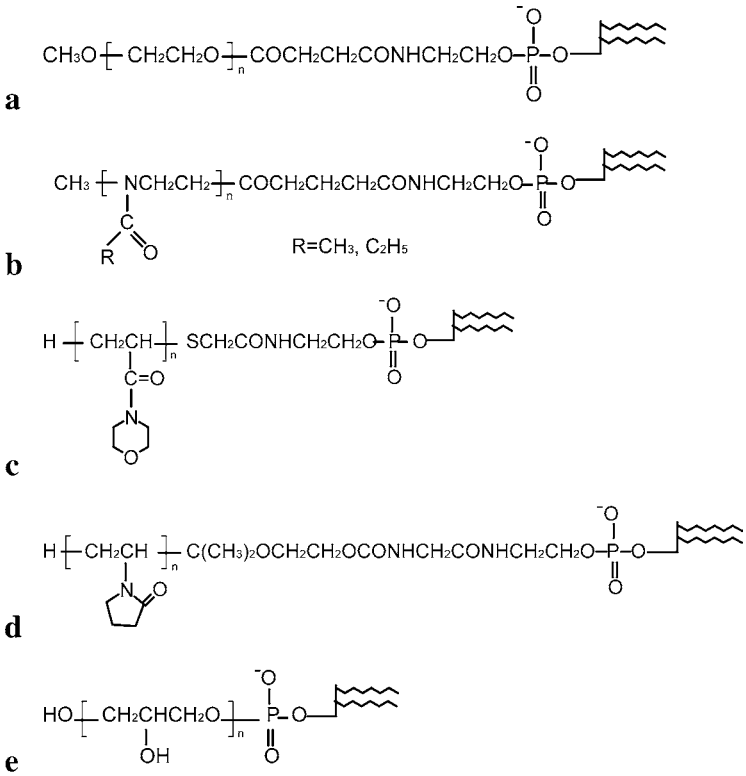

Scheme 8. (a) PEG–phosphatidyl ethanolamine; (b) poly(2-alkyl-2-oxazoline)–phosphatidyl ethanolamine; (c) poly(acryloyl morpholine)–phosphatidyl ethanolamine; (d) poly(vinylpyrrolidone)– phosphatidyl ethanolamine; and (e) polyglycerol–phosphatidyl–glycerol.

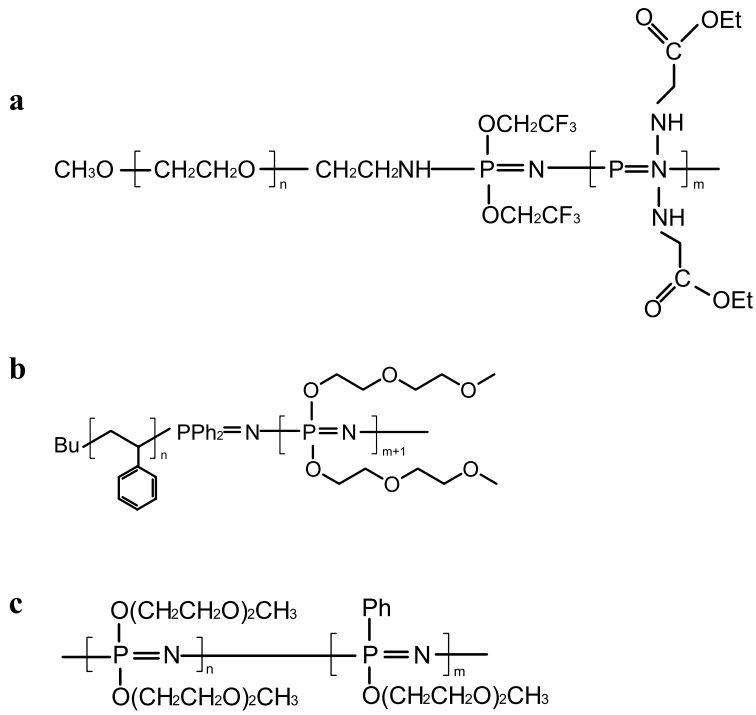

Scheme 9. (a) Block copolymer composed of PEG, poly[bis(ethyl glycinat-*N*-yl) phosphazene], and poly[bis(trifluoroethoxy) phosphazene]; (b) polystyrene-*b*-poly-[bis(methoxyethoxyethoxy) phosphazene]; and (c) methoxyethoxyethoxyl group (MEEP)–phenyl/MEEP copolyphosphazene.

mer, creating a newborn hydrophobic domain in which drug can be loaded. The PIC was totally water-soluble, and the size distribution was extremely narrow.

Architecture–Properties Relationship

From a chemistry standpoint, it is feasible to synthesize various block copolymers that form a micelle. When such a micelle is used as a drug carrier in the body, many performance-related issues must be addressed, including its static and dynamic stability, morphology, size and size distribution, biocompatibility, drug-loading capacity, release rate, circulation time, biodistribution, and endocytosis mechanism. To a large extent, these properties are determined by the architecture of the block copolymer.

Shape

Micellization is a procedure that minimizes the free energy of an amphiphilic polymer solution through the formation of selectively ordered structures. In the past years, a large number of diblock polymer AB or triblock polymer ABA have been proven to self-assemble micelles in a good solvent for the A block. In general, when the soluble block exceeds the length of the insoluble block, the particle assumes a core/shell spherical form, evidenced by atomic force microscopy (AFM), dynamic light scattering (DLS), and regular and cryo-transmission electron microscopy (TEM) (70). On the other hand, highly asymmetric diblocks containing long insoluble blocks and very short soluble blocks can be hardly dissolved in water to form micelle. A special preparation is required that involves copolymer dissolution in a certain organic solvent, followed by the gradual addition of water. These micelles, consisting of a hydrophobic core of the insoluble block surrounded by a thin shell of the soluble block, are called "crew-cut" micelles. Halperin (72) first proposed this term in 1990, but it was Zhang and Eisenberg (73) and Yu and Eisenberg (74) who carried out systematic experimental studies using PSt–*b*-poly(acrylic acid) (PSt–*b*-PAA), PSt–*b*-PEO, and PSt–*b*-poly-(4-vinylpyrinium methyl iodide) (PSt–*b*-P4VPMeI) micelles. A transfer to ellipsoid, rod, and lamellar micelles may occur when altering the copolymer concentration, type, and concentration of electrolytes in the medium, temperature, organic solvent, and the method of micelle preparation, which have also been extensively studied by Zhang and Eisenberg (75) and Zhang *et al.* (76). The influence of the proportion of the core- to shell-forming blocks on the aggregation shape will be further discussed in Polymersomes.

Critical Micelle Concentration and Size

A critical micelle concentration (CMC) value is the minimum concentration of a copolymer that will result in micelle formation. This parameter is a very critical indicator of micellization ability and micelle stability: the lower the CMC value, the easier the formation of micelle, and the more stable the micelle. Micelles are subject to extreme dilution upon intravenous injection into humans. If kinetically stable, slower dissociation allows polymeric micelles to retain their integrity and perhaps drug content while circulating in the

blood above or even below CMC for some time. Thus, a lower CMC can warrant the micelle to retain its original morphology until reaching the target site, which is a significant advantage of amphiphilic polymers over small molecular surfactants. CMC can be effectively measured using the fluorescent probe method. The most popular free probe is pyrene owing to its very low solubility in water (about 5×10^{-7} M), its long lifetime (400 ns in hydrophobic media and 200 ns in water), and its sensitivity of emission and excitation spectra to the polarity of its environment.

The size of the micelle is another critical factor that should be taken into account. Long circulation times of micelle are prerequisite to achieve depot effect. The high molecular weight of polymeric micelles ($>10^6$ g/mol) can ultimately prevent renal elimination unless the micelle dissociates to unimers. On the other hand, supramolecular structures with sufficient stability often end up accumulating in the liver and spleen because of their large size or protein adsorption, both triggering a rapid uptake by the RES. For this reason, drug delivery to organs other than the liver and spleen is limited for such carriers. Delivery systems that are smaller than 200 nm can reduce uptake by the RES, prolong the circulation time in the blood, and facilitate the extravasation from the leaky capillaries (77).

So far, researchers have disclosed the noticed influence of polymer architecture on CMC value and size of micelle. Taking PEG–PLA and PEG–PCL diblock copolymers as examples, it is observed that the CMC values of these polymeric micelles are extremely low (~1.0 mg/l) and exhibit a good inverse correlation with the weight ratio of the PLA or PCL segment to the PEG segment in block copolymers. Also, particle size and size distribution decline with an increase in the weight percent of the PLA segment (78,79). Analogously, the CMCs of PSt–PMEEP were determined as 1.8, 2.3, 10.0, and 13.6 mg/l with PSt/PMEEP ratios of 1:0.37, 1:0.58, 1:0.70, and 1:0.86, respectively (63). A set of amphiphilic PVP attached to palmityl or stearyl with MW between 1500 and 8000 Da was synthesized (59,80). Increasing the length of the PVP block also increased the CMC value and rendered the particle size bigger. Domeselaar *et al.* (81) recently described a simple but versatile solid-phase peptide synthesis method for preparing micelle-forming PEO–*b*-peptide for drug delivery. The CMC values for variable lengths of PEO–*b*-polytyrosine decreased as the length of the hydrophobic block increased.

Although it is true that for the majority of block copolymers, increasing the hydrophobic block chain length will decrease the CMC but increase the micelle size if the composition of chain is constant, it should be kept in mind that this rule is not universal to all cases because the interactions between the various chemical groups are so complicated and influenced by many factors. For instance, there is an apparent tendency of CMC values to decrease from 1.1×10^{-5} to 6.2×10^{-6} M when the MW of PEG increases from 750 to 5000 for PEG–(distearoyl)PE micelles (82). The similar phenomenon was found for block copolymer micelles composed of PEG–*b*-PLL (MW of PEG, 12,000) and a 20-mer oligonucleotide (ODN). When the degree of polymerization (DP) of PLL is 18, the micelles have a hydrodynamic radius of 24 nm, whereas with a longer PLL segment (DP of PLL 78), the radius is 37 nm (83). The dependence of micelle size on chain length is contrary to the conventional tendency, which can probably be explained by an increased repulsion when the chain gains more charges. On the other hand, there are several micelle systems whose size is constant regardless of the chain length, such as PEG–*b*-P(Asp)/PLL and PEG–*b*-PLL/plasmid DNA complex micelles (71,84).

Drug Encapsulation

There are two methods to load drugs: physical and chemical encapsulation. The latter is carried out by forming a drug–polymer conjugate core in the micelle as described in Types of Polymeric Micelle. Compared to chemical encapsulation, the physical encapsulation of drugs within the polymeric micelle core is more attractive because many polymers and drug molecules do not bear reactive functional groups, and the pharmacological effectiveness of the drug is maintained without chemical modification. Physical encapsulation usually operates through dialysis or O/W emulsion methods. Parameters including solvent type, concentration, and duration can affect the morphology of the micelles and its drug encapsulation. It is worth noting that polymer architecture also greatly influences drug encapsulation. The solubilization capacities of two micelles separately made from diblock PEG–*b*-poly(styrene oxide) and PEG–*b*-poly(1,2-butylene oxide) have been compared using a poorly water-soluble drug, griseofulvin (85). The results showed that the solubilization capacity of the same drug in a PEG–*b*-poly(styrene oxide) micelle was approximately four times that of PEG–*b*-poly(1,2-butylene oxide) because of the increased hydrophobicity of poly(styrene oxide) block. Micelles of PEG–*b*-PDLLA were investigated for their drug-loading ability for a hydrophobic drug, paclitaxel. Similarly, it was found that the loading weight portion of paclitaxel in PEO–*b*-PDLLA micelles reached 25% and its solubility increased 5000-fold, which contrasts with the loading of 0.5% in Pluronic micelles because of higher hydrophobicity and T_g of the PDLLA block (86). Furthermore, the solubilization test indicated that the loading content of Sudan black B in the micelle was 63.9%, whereas that of testosterone was only 0.74%, considering the higher hydrophobicity of Sudan black B (87). However, when PEO–*b*-PLA micelle was used to load a water-soluble drug, the length of PLA block seemed not to affect their encapsulation properties (88). Therefore, it is reasonable to conclude that drug encapsulation mainly relies on the intrinsic interaction affinity between drug and certain groups of hydrophobic block.

Biodistribution

Biodistribution in the body is an integrative problem related to the size, CMC, surface charge, and the targeting moiety of the micelle. As discussed in Critical Micelle Concentration and Size, low CMC and small size can insure shape integrality to retain the drug and extend the circulation time of micelle, which facilitates the accumulation of drug-loaded micelle and subsequent drug release at the target site. In addition, surface charge is another predominant factor that affects micelle biodistribution. Having an electrically

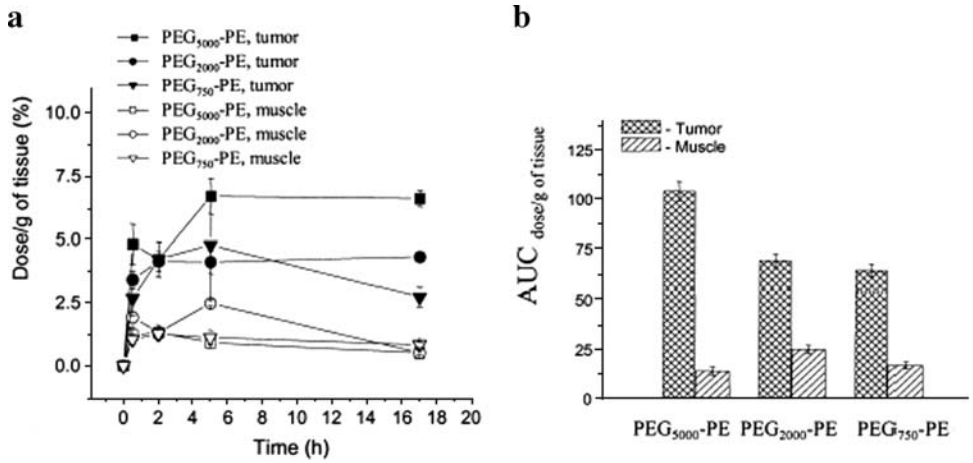

Fig. 8. Selective accumulation of PEG–PE micelles in Lewis lung carcinoma tumor in mice: (a) pharmacokinetics; (b) area under the curve (AUC) (89).

neutral surface on the micelle should suppress the unspecific uptake. Incorporating drugs into "stealthy" micelles, which present a hydrophilic shell such as PEG, is the most effective method to prolong plasma half-lives of the drugs by reducing interactions with the blood components and RES uptake. Additionally, the molecular weight of PEG has proven to remarkably affect biodistribution. For example, when the accumulation pattern of PEG–PE micelles with varying PEG MW was evaluated, it was found that the highest MW PEG used in the tested micelles resulted in the largest total tumor uptake in an Lewis lung carcinoma tumor model (Fig. 8) (89). Conversely, PEG–distearoylphosphatidylethanolamine micelles using lower MW PEG (smaller size) exhibited slightly better accumulation in another murine tumor model, EL4 T cell lymphoma (Fig. 9) (90). These results were possibly associated with the cutoff size of the tumor vasculature. Kakizawa and Kataoka (91) specially illustrated the effect of surface charge on micelle biodistribution for gene delivery in their review because positively charged blocks are necessary to complex with plasmid DNAs or ODNs. PEG coating also keeps polycation/DNA complexes in the blood for a longer time period and also enhances the micelle stability, leading to improved gene delivery efficiency. In such systems, N/P ratio is an important parameter, which not only determines the ζ-potential of the micelle but is also relevant to the stability of polycation/DNA complex. In Agarwal's study, the rate of DNase degradation decreased significantly upon addition of a cationic pentablock copolymer of poly(diethylaminoethylmethacrylate) (PDEAEM), PEO, and PPO (PDEAEM–PEO–PPO–PEO–PDEAEM) (Scheme 10) to the DNA solution. At or above N/P ratios of 8:1, scarce change in absorbance was detected upon addition of DNase I, suggesting the polymer protective action to DNA (Fig. 10) (92).

Biodistribution actually implies two strategies, i.e., the systemic level as mentioned above and the cellular levels. Macromolecular entities cannot diffuse through the cellular membrane but can be internalized inside the cells through endocytosis. Three types of endocytosis mechanism have been discovered including fluid-phase endocytosis, adsorptive endocytosis, and receptor-mediated endocytosis (RME), which are explained in the review by Kakizawa and Kataoka (91). It is well established that micelles with a positive surface charge can be effectively taken up by adsorptive endocytosis through electrostatic interactions with the negatively charged cell membrane. Fluid-phase endocytosis has a lower internalization rate compared to adsorptive endocytosis. The RME requires specific ligand moieties to be installed on the micelle surfaces. In addition, the hydrophilic block plays an indispensable role in facilitating endocytosis of the micelle.

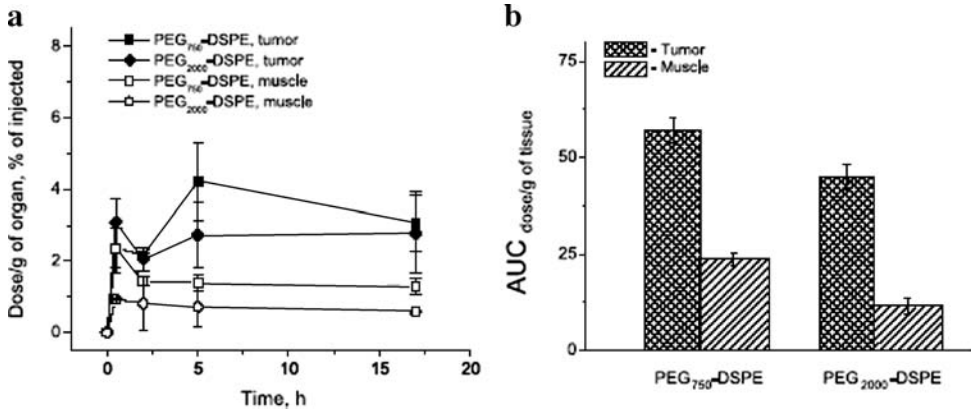

Fig. 9. Selective accumulation of PEG–PE micelles in EL4 T lymphoma tumor in mice: (a) pharmacokinetics; (b) AUC (90).

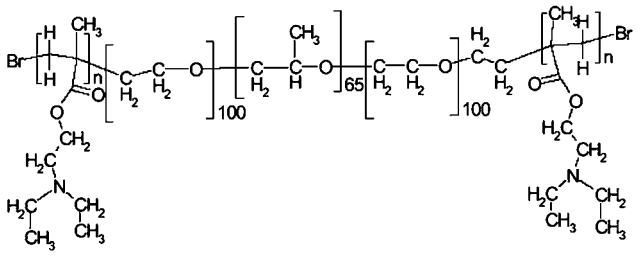

Scheme 10. Cationic pentablock copolymer of poly(diethylaminoethylmethacrylate), PEO, and poly(propylene oxide).

For example, the molecular weight of PEG was shown to be important in mediating transfection for PEG–*g*-PLL micelle with folate attached at the end of the PEG segments. A significant enhancement of transfection was reported when the MW of PEG exceeded 3400 (93). The addition of a PEG spacer (MW 3400) between folate and PLL provided a 74-fold increase in the transfection efficacy compared with binding folate directly to PLL in view of the steric effects of targeting moiety.

Drug Release

Typically, a drug exerts its action only after it releases from the micelle core. But this does not mean the quick drug release rate is optimal; otherwise, there would be serious drug loss during circulation. Lavasanifar *et al.* (77) addressed some factors to control the drug release from micelles in their review. When drugs are physically encapsulated in stable polymeric micelles, the drug release rate is controlled by the diffusion out of the micelle core and/or by dissociation of the micelles. The diffusion rate may be quite low if the drug prefers to interact with the core-forming block. The design of block copolymer micelles with glassy cores under physiological conditions (37°C) also favors release in a sustained manner. PSt and poly(*t*-butyl acrylate) cores in a rigid state have been proposed to reduce the release of pyrene from a micellar carrier (94). The release rate of the encapsulant from the micelle is accelerated with an increased content of PEG but delayed with more hydrophobic chains (95). The localization of the solute in the core/shell structure, micellar size, and molecular volume of the drug are other factors that also influence the rate of drug diffusion from the polymeric carrier.

More attractive examples in this case refer to the pH-sensitive micelles, thermosensitive micelles, and reversibly cross-linked micelles. Based on the fact that many pathological processes in various tissues and organs are accompanied by local acidosis or temperature increases, pH-sensitive or thermosensitive micelles can be designed to achieve targeted drug release. The Bae group (96,97) has developed several kinds of pH-sensitive micelles, e.g., poly(L-lactide)/PEG–polysulfonamide (PLLA/PEG–PSD) and poly(L-histidine)–PEG (polyHis–*b*-PEG; Scheme 11), and established new drug release mechanisms triggered by the sharp solubility transition of carriers at tumor pH. Sulfonamide is a weak acid and its solubility in water decreases within a narrow pH range (−0.2 pH units). PLLA/PEG–PSD micelles were stable with a unimodal size distribution and aggregated below a pH of 7.0 owing to the deionized SD on the micelle surface, which resulted in the loaded drug being squeezed out at a lower pH. The drug release mechanism of polyHis–*b*-PEG is totally different. As shown in Fig. 11, the CMC of polyHis5k–*b*-PEG2k micelle was significantly elevated below a pH of 7.2 because the protonation of the imidazole group in the polyHis at a lower pH caused a reduction in hydrophobicity. Below a pH of 5.0, the CMC could not be detected, suggesting failure in micelle formation. Consequently, below the critical pH for destabilization of a micelle, Dox release was greatly accelerated. Because of this complete disintegration after reaching the target site, such pH-triggered micelles

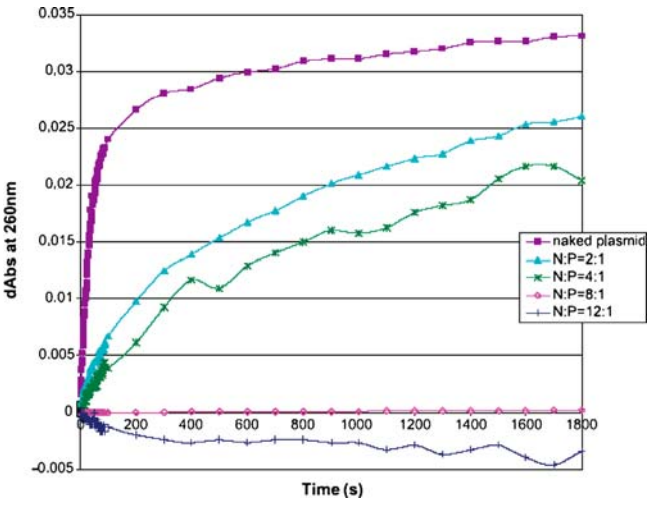

Fig. 10. Nuclease resistance of polyplexes against DNase I activity at different N/P ratios. An amount of 20 μg of DNA/ml final concentration was used, and each sample was incubated with 5 IU DNase I/μg DNA (92).

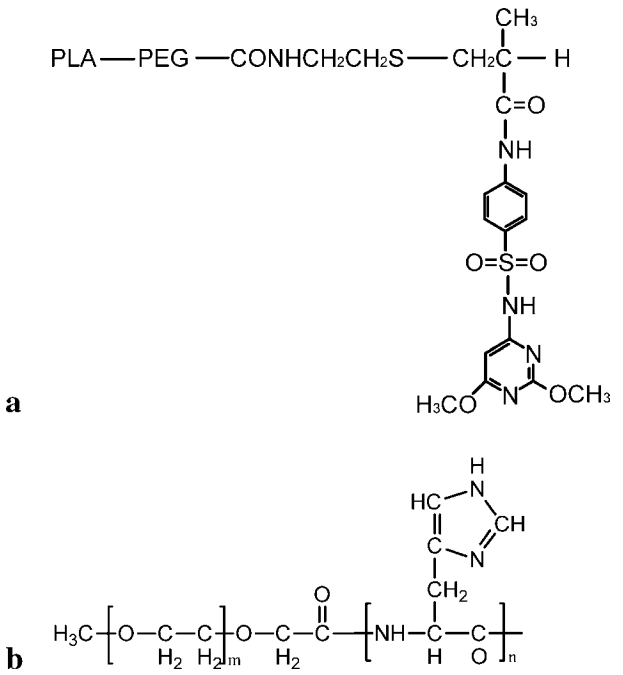

Scheme 11. (a) Poly(L-lactide)–PEG–polysulfonamide and (b) poly(L-histidine)–PEG.

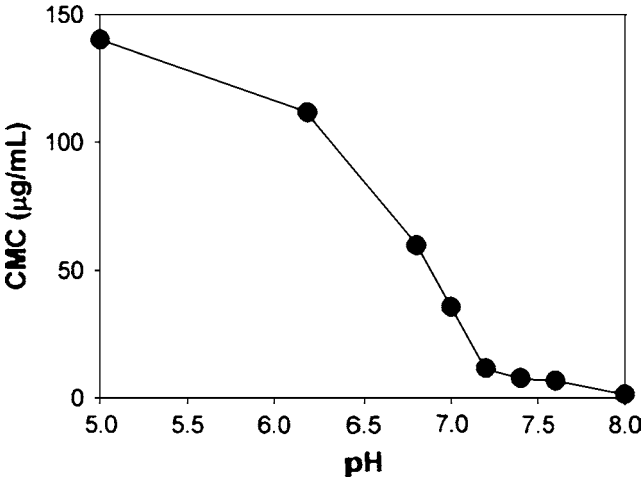

Fig. 11. The pH effect on the critical micelle concentration (CMC) of polyHis5k–*b*-PEG2K polymeric micelles that were prepared at various pH values (pH 8.0–5.0) (97).

were supposed to improve the targeting effect of a multiple dose administration. Okano *et al.* (98–100) have studied thermosensitive micelles using polyNIPAAm (PNIPAAm) as the thermoresponsive outer shell-forming block and PDLLA or poly(*n*-butyl methacrylate) for the hydrophobic inner core. Drug release can be enhanced when higher temperatures beyond the lower critical solution temperature (LCST) of PNIPAAm induce the shrinkage of the outer shell. In addition, both drug release and *in vitro* cytotoxicity showed a reversible thermoresponsive on/off switching behavior to temperature change. These micelles can achieve both spatial and temporal control for drug release. Interestingly, Kakizawa *et al.* (101,102) explored a reversibly cross-linkable micelle. They first introduced thiol groups into a small number (10–20%) of lysine repeat units in PEG–*b*-PLL and formed PIC micelles with a negatively charge electrolyte, such as an ODN or Pasp. Automatic oxidation of the thiols to disulfide bonds resulted in cross-linking of the micelle's hydrophobic core to stabilize the association of ODN or other loaded drugs. By taking advantage of the breaking of disulfide cross-links in cells containing abundant reducing agents such as dithiothreitol or glutathione, a promising carrier for targeting drug delivery using a triggering drug release mechanism of micelle reverse instability can be achieved.

In the case of drug conjugates, the covalent bonds between therapeutic molecules and polymers have to be cleaved for drug release. Because water penetration into hydrophobic and rigid cores may be restricted, drug release depends on the rate of micellar dissociation and the breakup of the labile bonds as well. For a PEG–*b*-PAsp micelle loaded with CDDP, increasing the PAsp content led to prolonged release of CDDP, owing to the stronger interaction between PAsp and CDDP (103).

Triblock Copolymers

Assuming constant chain length and composition, the aggregation of BAB block copolymer, generally, is more difficult than that of AB and ABA block copolymer in a good solvent for block A. Relatively few studies have dealt with the aggregate properties of the BAB block copolymer in water. Yuan *et al.* (104) synthesized a series of PSt–*b*-PEG–*b*-PSt by atom transfer radical polymerization (ATRP). It was found that the ordinary dialysis method is applicable to form micelle in the water only for copolymers with a relatively high PEG content (93%) and low total molecular weight (10,800; PSt_4–*b*-PEG_{227}–*b*-PSt_4; the numbers represent DP). When the content of PEG became quite low, i.e., the insoluble PSt block length was longer than the soluble PEG block (PSt_{43}–*b*-PEO_{45}–*b*-PSt_{43} and PSt_{18}–*b*-PEO_{45}–*b*-PSt_{18}), it was difficult to prepare micelle by dialyzing a polymer organic solution against water. Thus, an innovative method was employed to construct the micelle; that is, the polymers were first dissolved in dimethylformamide (DMF), then twice-distilled water was added dropwise, and lastly, DMF was dialyzed off. The resultant polymeric micelle belongs to a family of "crew-cut"-shaped aggregates (105). In addition, they found an interesting phenomenon for PSt_4–*b*-PEO_{227}–*b*-PSt_4 in that the size polydispersity was very high. As discussed above, micelles made from the block copolymers with a relatively large soluble block have a spherical shape and a narrow size distribution. In view of the architecture of BAB triblock polymers, it has been currently accepted that the aggregation occurred through the linking of primary micelles by chain ends from different micelles (Fig. 12). This theory distinguishes the micelle model of BAB from that of AB- or ABA-type block copolymers. Hence, it is not difficult to understand the fact that for a composition of PCL–*b*-PEG–*b*-PCL, micelle size increased when the ratio of PCL to PEG became higher (106). In fact, BAB triblock polymers are often used to fabricate hydrophobic drug vehicles. The introduction of hydrophilic block A is simply to modulate the degradation of the whole polymer.

ABA triblock copolymer can also construct self-assembled micelles, but the reason why they have attracted progressing interest for controlled drug release is their thermosensitive sol–gel reversible character. The commercial PEO–*b*-PPO–*b*-PEO product, Pluronic (BASF) or Poloxamer (ICI) series, with various molecular weights and PEO/PPO block ratios has been widely used as a nonionic surfactant. Aqueous solutions of some Poloxamers would experience phase transition from sol to gel and to sol as the

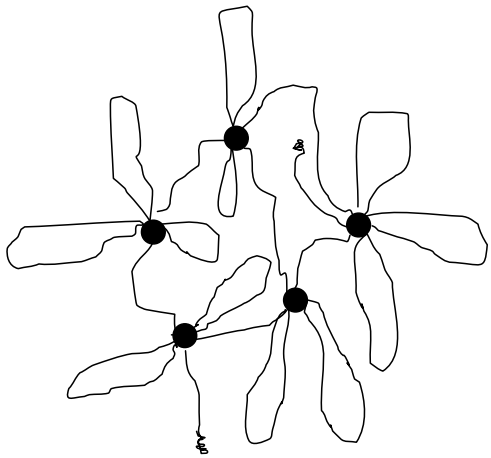

Fig. 12. The aggregated micelle of PSt4–*b*-PEO227–*b*-PSt4 in aqueous solution (104).

temperature was increased monotonically when polymer concentrations were above a critical value. These properties have been utilized to fabricate *in situ* gelating subcutaneous injections to achieve sustained drug release or create scaffolds for cell immobilization and tissue regeneration. However, because the gel dissociates in water, Poloxamers can be used only for a short time period, within a single day. In 1997, a novel triblock copolymer (PEG–*b*-PLLA–*b*-PEG), which combined thermogelation, biodegradability, and no toxicity, was introduced. Different from Poloxamer, PEG–*b*-PLLA–*b*-PEG exhibited a single sol-to-gel transition in water with decreasing temperature. The gelation concentration (10–30 wt.%) and temperature (20–60°C) were influenced by the length of the PLLA block when the terminal PEG block was kept constant. When PLLA was replaced by PLGA as the hydrophobic blocks in the triblock copolymer, a noteworthy phenomenon happened. PEG–*b*-PLGA–*b*-PEG dissolved in water at room temperature and became a gel at body temperature. Both the sol–gel transition temperature (ΔT) and the critical gel concentration (CGC) could be controlled by changing molecular parameters of PEG–*b*-PLGA–*b*-PEG triblock copolymers, such as the PLGA length, the PEG length, and the ratio DLLA to GA in the middle, which was reviewed by Jeong *et al.* (107). This triblock polymer formed an *in situ* gel at the body temperature, which retains its integrity for more than 1 month. However, the PEG–*b*-PLGA–*b*-PEG copolymer forms sticky paste and cannot be lyophilized into a powder, bringing about some difficulty for weighing and transfer. Particularly, it takes several hours to dissolve it into aqueous media to prepare an injection. In 2005, a new Poloxamer analog PEG–*b*-PCL–*b*-PEG was synthesized (108). This is a powder at or below room temperature, so it is convenient to handle and easily lyophilized to powder form. Moreover, it can be quickly dissolved in water, which is practical for clinic use. The phase transition of PEG–*b*-PCL–*b*-PEG triblock copolymer aqueous solution was similar to that of the PEG–*b*-PLGA–*b*-PEG aqueous solution except for the presence of a transparent sol phase around 52.5–53°C when the concentration of the PEG–PCL–PEG was greater than 25%. When the concentration of the polymer was less than 25%, the upper sol was turbid, similar to the PEG–*b*-PLGA–*b*-PEG. Parameters related to the particular application, including CGC and ΔT, can be controlled by varying the molecular weight of each block.

Polymersomes

Amphiphilic block copolymers form a range of self-assembled aggregates including spherical, rod-like, tubular micelles, lamellae, or vesicles, depending on polymer architecture and preparation conditions. Polymer vesicles having a liposome-like structure with a hydrophobic polymer membrane and hydrophilic inner cavity are called polymersomes (peptosome if one block of the copolymer is peptide) (109). The polymersomes offer some advantages over liposomes, not only in vesicle stability but also in the regulation of membrane thickness. Current polymersome research involves quite diverse fields such as drug delivery system, transfection vectors, protective shells for sensitive enzymes, and microreactors (110,111).

Phospholipids can array into a bilayer membrane. Analogously, block copolymers can also assemble into a bilayer as described in Fig. 13a. The polymeric bilayer is a unique structure composed mostly of diblock copolymer-based vesicles. The recent development of amphiphilic block copolymers for polymersome construction has been reviewed (112). In general, amorphous hydrophobic blocks with a low glass transition (T_g) temperature are optimal for constructing a lipid-like membrane with fluidity. Typically, hydrophobic blocks are poly(ethyl ethylene) (PEE) and polybutadiene (PBD), which can be cross-linked subsequently to enhance stability (113). Biodegradable PLA and PCL have been utilized considering the need for disposal *in vivo* and controlled drug release (114). Hydrophilic blocks involve nonionic PEG and charged poly(acrylic acid) and various peptides.

It has been proved that triblock copolymers can also form polymersomes, but thus far, very few studies have been able to clarify the molecular conformation of the hydrophobic membrane. Taking the molecular symmetry of triblock copolymers into account, a diversiform model mixing U-shaped (two hydrophilic chains on the same side of the membrane) and I-shaped (two hydrophilic chains on the two sides of the membrane) forms is proposed (Fig. 13b), derived from the structure of Langmuir film (115). More works will be needed in the future to validate this assumption. Recently, Brannan and Bates (116) synthesized a novel ABCA tetrablock copolymer, PEO–*b*-PSt–*b*-PBD–*b*-PEO (OSBO), and studied polymersome dimensions via cryo-TEM using osmium tetroxide solution staining. It is noteworthy that the polymersome membrane structure changed with the PEO content (W_0) in the copolymer (Fig. 14). When $W_0 < 0.5$, a complexed hydrophobic membrane is observed, characterized by two levels of core contrast: the inner dark layer for PB and the outer light for PSt. As $W_0 > 0.5$, however, the dyeing distribution in the vesicle represented a completely different feature. Herein, the water compatibility of each hydrophobic block as well as the chain architecture should be considered.

In cases where block copolymers contain PEO, the amount of PEO is considered to be a predominant factor in

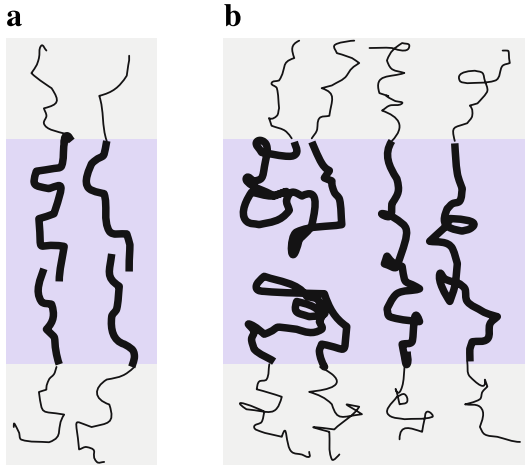

Fig. 13. Molecular assembly modes for polymersome based on (a) diblock copolymer: bilayer form, and (b) triblock copolymer: mixing U-shaped and I-shaped forms.

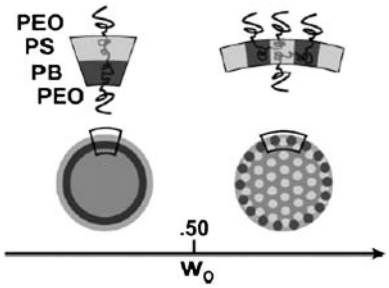

Fig. 14. Structural models for vesicles above and below the morphological transition composition (116).

determining the supramolecular formation of block polymers into micelles, or in vesicles, or something else. As usual, increasing the weight fraction of PEO (f_{EO}) in the copolymer will result in the tendency to form curved micelles rather than stable polymersomes. Take the diblock copolymer PEO–PLA as an example (114). When smaller hydrophilic PEG fractions of $f_{EO} < 20\%$ were used, the copolymer exhibited a strong propensity to form solid-like particles. Increasing f_{EO} to ~20–42% generally switched the assembly to a polymersome. After further increasing the f_{EO} to within 42 and 50%, both worm micelles and some spherical micelles were observed. Above a f_{EO} of 50%, spherical micelles are primarily noticed. Figure 15 illustrates the conformation transform of PEG–PLA from cylinder to cone shape, which clearly explains the relationship between the f_{EO} and the assembled structure (114). Yu and Eisenberg reported the relationship between the block ratio and the morphology of PS–*b*-PAA crew-cut aggregates. Using dioxane as the organic solvent to dissolve the copolymer in the preparation process, aggregates of spheres, cylinders, or vesicles were obtained, respectively, when the corresponding ratio of hydrophilic PAA block was 26.0, 15.1, or 10.4 mol% (117). A similar phenomenon was observed in the study on the ABCA-type block copolymer OSBO (116). Using the film rehydration method, OSBO-36 (the number refers to f_{EO}%) and OSBO-

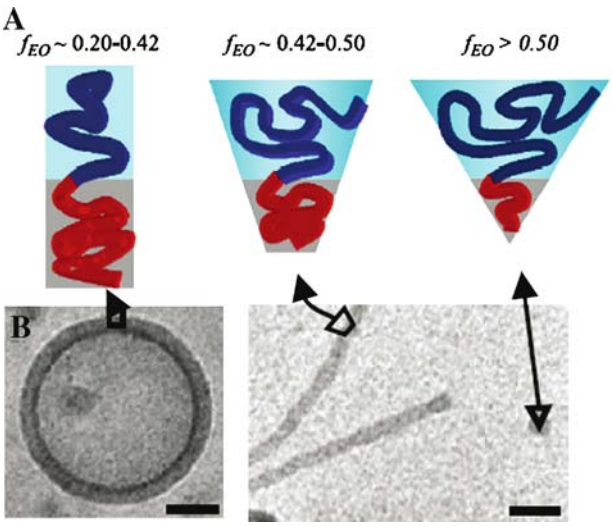

Fig. 15. The relationship between copolymer conformation and resulting shape of PEO–PLA self-assemblies as a function of PEO fraction (f_{EO}). (A) Illustration of copolymer chains molecular, and (B) cryo-transmission electron microscopic images of morphologies (114).

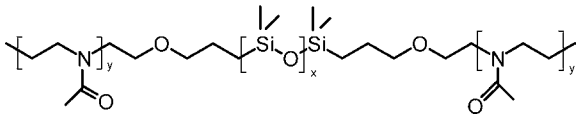

Scheme 12. Poly(2-methyloxazoline-*block*-dimethyl-siloxane-*block*-2-methyl oxazoline).

46 almost exclusively formed vesicles in the water, whereas OSBO-52 and OSBO-66 had some cylindrical micelles accompanying a minority population of polymersomes. The f_{EO} of 0.5 is regarded as the boundary where polymersomes switch to micelles. For ABA-type amphiphilic poly(2-methyloxazoline-*block*-dimethyl-siloxane-*block*-2-methyl oxazoline) (PMOXA-*b*-PDMS-*b*-PMOXA; Scheme 12) (118), the morphology of self-assemblies was largely controlled by the weight ratio of hydrophobic PDMS to hydrophilic PMOXA. A ratio below 1.5 favored the vesicle formation, above which the tendency to form nanotube became obvious.

The thickness of the polymersome membrane is obviously influenced by the length of the hydrophobic chain in the copolymer (119,120). For example, in the system of PEO–PBD (Scheme 13), the hydrophobic membrane thickness (d) increased from 9.6, 10.6, to 14.8 nm when the molecular weight of BD increased from 3600 to 5200 to 10,400 g/mol (121). Likewise, in other series of PEO–*b*-PBD, d was gradually enhanced from 8–9, 9–10, to 12–13 nm with the increase in MW of BD from 1.8, 2.5, to 5 kDa (122).

Instead of directly dissolving block copolymer in water, specific techniques are generally required to fabricate polymersomes. Electroformation has proved to be the most useful method for preparing the giant polymeric vesicles with diameters in the range of 10–200 μm. In this process, a thin film of polymer on adjacent electrodes is phoresed by alternating current into an aqueous solution (123,124). Vesicle size can be readily controlled by varying the voltage and frequency of the electric field. As for nanoscaled polymersomes, film rehydration is preferred, just like the typical preparation method for liposomes (125). The polymer is dissolved in a certain volatile solvent such as chloroform or tetrahydrofolate and dried in a round-bottom flask by rotary evaporation of the solvents to obtain a thin polymer film. The addition of water or buffer to the flask will lead to spontaneous budding of vesicles off the round-bottom glass surface into solution. The size and size distribution of polymersomes can be regulated by further sonication or extrusion or even with several freeze–thaw cycles. Another method is called injection, where the organic polymer solution is slowly injected into an aqueous solution to precipitate the polymersome (126). Sometimes, adding water directly into the organic polymer solution is also useful (127).

HYPERBRANCHED POLYMERS

A typical example of a branched polymer used in drug delivery systems is PEI, a large family of water-soluble

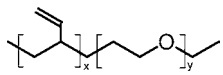

Scheme 13. Poly(ethyl ethylene)-*b*-polybutadiene.

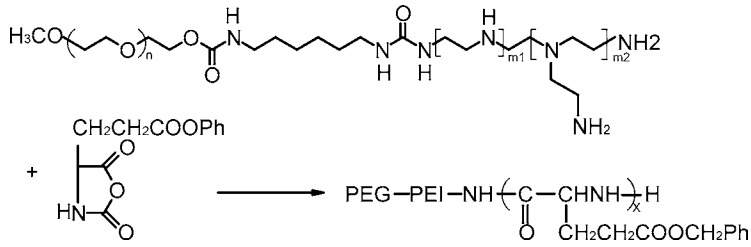

Scheme 14. Synthesis of PEG–*b*-PEI–*b*-poly(γ-benzyl L-glutamate).

polyamines with varying molecular weights and degrees of chemical modification. Extensive progress has been made in understanding the polymerization mechanism, control of polymer branching, and alternative routes to these polymers. This branching polymer presumably yields spheroid-shaped molecules possessing primary, secondary, and tertiary charged amine groups. PEI can function as a cationic polyelectrolyte and strongly attracts anionically charged organic and inorganic materials, colloids, and surfaces, which leads to its extensive applications for anionic DNA delivery. A series of graft copolymers based on hyperbranched PEI (hy-PEI) with nonionic and hydrophilic block were synthesized, where the task of PEI was to condense nucleic acids, while the hydrophilic block was supposed to increase the solubility of the interpolyelectrolyte complex and stabilize it against opsonization.

Two series of PEI–*g*-PEG copolymers were synthesized using an elegant two-step method; one series contained a grafted PEI (MW 25,000) with varying numbers of PEG (MW 5000), and the other series contained equal amounts of PEI and varying MW PEG (128). In the first series, cytotoxicity was reduced as the graft number of PEG increased, and in the second series, an increase in the MW of PEG from 550 to 20,000 significantly increased the cytotoxicity, suggesting that excessive membrane destruction always occurs when the cationic domain is accessible.

Shuai *et al.* (129) prepared the biodegradable amphiphilic copolymer (hy-PEI–*g*-PCL–*b*-PEG) by grafting activated PCL–*b*-PEG onto hy-PEI. Complexation of plasmid DNA with various copolymers created particles of 200 nm in diameter. Copolymer composition was found to significantly affect the gene transfection efficiency of polyplexes in that lower graft density and higher molecular weight PEI favored higher gene transfection efficiency.

More recently, the micelle character of biodegradable PEG–*b*-PEI–*b*-poly(γ-benzyl L-glutamate) (PBLG; Scheme 14) was investigated (130). The copolymer self-assembled in water with CMC in the range of 0.00368–0.0125 g/l depending on the hydrophobic block content in the copolymer and the ionic state of PEI. The CMC decreased when the PBLG block content was increased. Micelle size decreased and CMC increased simultaneously, depending on the protonated degree of PEI through the addition of HCl.

Novel amphiphilic scorpion-like macromolecules (AScMs; Scheme 15) were designed comprising acylation of mucic acid with acyl chlorides of varying chain lengths as the branched hydrophobic domains whereas PEG as hydrophilic domains (131,132). Low CMC values (10^{-5}–10^{-7} mol/l) and small particle sizes (10–20 nm) of AScMs were observed. Furthermore, the CMC and the particle size can be well controlled by the length of PEG or acyl chains. These unique properties of AScMs will be useful for encapsulating and delivering lipophilic drugs. Later, Frauchiger *et al.* (133) and Djordjevic *et al.* (134) constructed a novel amphiphilic starlike macromolecule (Scheme 16) by simply taking advantage of this vagarious branched polymer and greatly approved of its potential to work as a drug carrier.

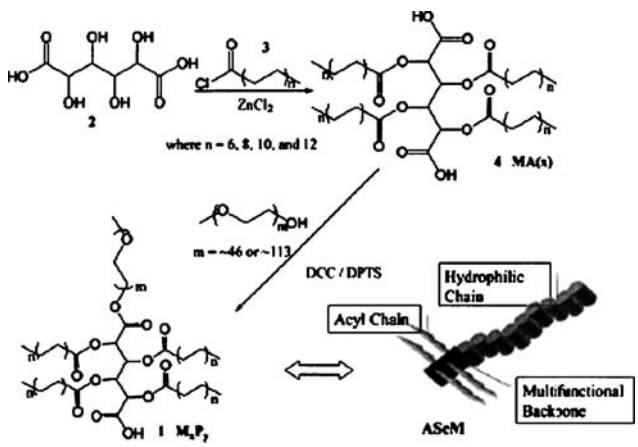

Scheme 15. Synthesis of amphiphilic scorpion-like macromolecule (AScM) (131).

Scheme 16. Amphiphilic starlike macromolecule composed of AScM.

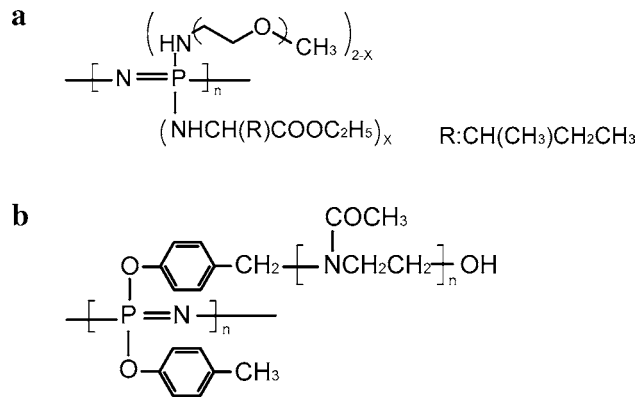

Scheme 17. (a) Graft polyphosphazenes bearing α-amino-ω-methoxy-PEG; (b) poly(4-methylphenoxy phosphazene)-*g*-poly(2-methyl-2-oxazoline).

GRAFT POLYMERS

Except for those like hy-PEI graft polymers, most graft polymers can also be called comb-type copolymers, which contain extensive branching along a linear polymer backbone. Two general methods have been applied to synthesize the graft polymers according to the properties of backbone and branching. One method refers to the direct copolymerization of two or more than two monomers, one of which must already have a branching (135). The other method uses the polymer as a backbone in the presence of polyfunctional active sites, which are used to couple with new branches or to initiate the propagation of branching (136). For example, Ito *et al.* (137) used a macromer technique to synthesize a graft copolymer of PSt with uniform PEG side chains. They obtained PEG macromers using potassium tertiary butoxide as the initiator and methacryloyl chloride or *p*-vinyl benzyl chloride as the terminating agent to obtain PSt–*g*-PEG. An apparent decrease in the reactivity of both PEG macromers and comonomers was ascribed to thermodynamic repulsion between the macromer and the backbone. On the other hand, Candau *et al.* (138) obtained PSt–*g*-PEG by reacting a living monofunctional PEG with a partly chloromethylated PSt backbone. Using this method, PSt needs to be activated first to form coupling sites for PEG.

When considering biodegradation along with the synthesis method, several water-soluble polymers are typically selected as the backbone for graft polymers, taking advantage of their multiple active groups along the backbone, such as chitosan, alginate, dextran, and poly(L-glutamic acid). PEG is the most popular side chain for these polymer backbones because it always facilitates the formation of thermosensitive gels. For example, when more than ~40 wt.% of PEG was grafted to chitosan chains via covalent bonding, the aqueous solution of the resultant copolymer was an injectable liquid at low temperature and transformed into a semisolid hydrogel at body temperature. After an initial burst release in the first 5 h, a steady linear release profile for a protein from the hydrogel was achieved for a period of ~70 h (139). PNIPAAm is another popular side chain with the aim to construct a thermosensitive gel because of its intrinsic water solubility change with temperature (140).

Recently, a number of reports have focused on the biodegradable graft polyphosphazene. Lee *et al.* (141) and Lee and Song (142) synthesized a series of graft polyphosphazenes bearing α-amino-ω-methoxy-PEG (AMPEG; Scheme 17a) and different hydrophobic amino acid esters, which exhibit reversible sol–gel properties. The gelation properties of the polymer were affected by several factors, such as the composition of substituents, the chain length of AMPEG, and the concentration of the polymer solutions. The more hydrophilic composition of polymers offered higher gelation temperatures. Increasing the chain length of AMPEG also gave higher gelation temperatures (Table II). In addition to thermosensitive gels, graft polyphosphazenes have also been modified to construct micelles in water. Poly(4-methylphenoxy phosphazene)-*g*-poly(2-methyl-2-oxazoline) (Scheme 17b) is a typical example, and its micelle characterization has proven to be related to the polymer architecture (143). When the graft ratio of poly(2-methyl-2-oxazoline) was held at 5%, the CMC was found to be 0.025%. Above CMC, the polymer solution showed surface tension of 46 dyn/cm. In the case of the 20% grafted polymer, the polymer also formed micelles but showed poor surfactant behavior with high surface tension (65 dyn/cm) above a CMC of 0.05%. It is noteworthy that Qiu's group synthesized several series of amphiphilic polyphosphazene–*g*-PNIPAAm containing hydrophobic amino acid esters or ethyl 4-aminobenzoate (Scheme 18) with different composition using macromolecular reaction. These graft polyphosphazenes exhibited thermosensitivity attributed to the property of PNIPAAm. Consequently, the polymers had the capability to form self-assembled nanoparticles at temperatures below

Table II. Characteristics of Poly(organophosphazenes) (141)

Polymer	Structure	T_{ass} (°C)[a]	T_{max} (°C)[b]	T_{LCST} (°C)[c]	V_{max} (Pa s)[d]	MW[e] (10^4)
1	$[NP(AMPEG350)_{0.87}(IleOEt)_{1.13}]_n$	7	29	37	116.9	3.9
2	$[NP(AMPEG350)_{1.06}(IleOEt)_{0.94}]_n$	11	38	55	28.6	2.1
3	$[NP(AMPEG350)_{1.45}(IleOEt)_{0.55}]_n$			74		6.0
4	$[NP(AMPEG550)_{0.76}(IleOEt)_{1.24}]_n$	35	61	75	5.0	2.0

[a] The association temperature at which the viscosity of the polymer solutions (10 wt.%) begins to increase sharply.
[b] The temperature at which the polymer solutions (10 wt.%) reach their maximum viscosity.
[c] The lower critical solution temperature (LCST) was identified as the temperature at which the polymer solutions (10 wt.%) became turbid.
[d] The viscosity of the polymer solutions at T_{max}.
[e] The molecular weight of the polymers was measured by GPC using tetrahydrofolate solutions containing 0.1% (w/v) tetrabutylammonium bromide.

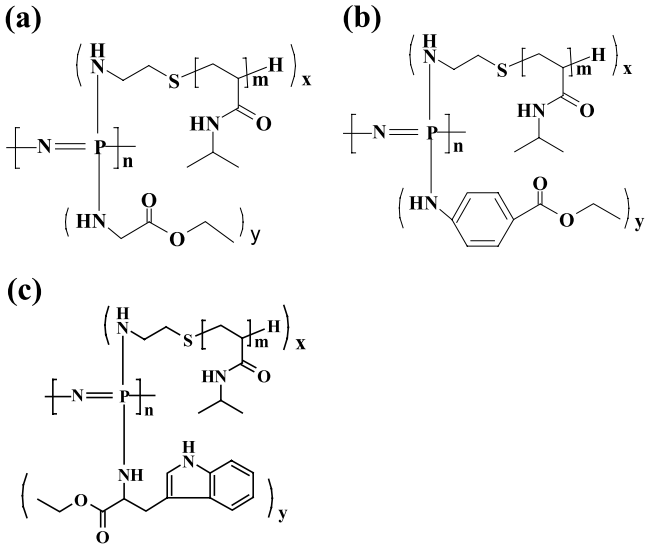

Scheme 18. Amphiphilic polyphosphazene-*g*-PNIPAAm containing various hydrophobic groups: (a) ethyl glycinate; (b) ethyl 4-aminobenzoate; (c) ethyl tryptophan.

LCST with the proper amount of grafted chains, whereas they aggregated once the temperature exceeded LCST (144,145). They further investigated the architecture–property relationships of those polymers in detail. The more hydrophobic groups a copolymer contained, the lower its LCST. Furthermore, the critical association concentration (CAC) of copolymers decreased by increasing the content of hydrophobic side groups (146). The effect of hydrophobic groups on CAC was similar to the amphiphilic block polymers discussed above. More recently, they achieved a novel amphiphilic polyphosphazene–*g*-PNIPAAm containing a unique fluorescence feature (Scheme 18c), which will facilitate the tracking of the fortune of drug-loaded nanoparticles in the body (147). Owing to the flexibility of this synthesis method, graft polyphosphazene offers a broad platform to design biomaterials with versatile adaptability for applications.

STAR POLYMERS

Star polymers have a three-dimensional hyperbranched structure where linear arms of the same or different molecular weight emanate from a central core. Star polymers can be produced either by arm-first or core-first methods (148). The arm-first method involves the use of a multifunctional termination agent or cross-linking of linear polymer chains prepared by living controlled polymerization. Georgiou *et al.* (149) reported that the synthesis of the arms of a star polymer was accomplished by group transfer polymerization of DMAEMA, initiated by a monofunctional initiator. Subsequently, cross-linking took place *in situ* by the polymerization of a bifunctional methacrylate, which led to interconnection of the "living" linear chains at one end to give an "arm-first" star polymer. In the core-first method, polymer chains are propagated from a multifunctional initiator. Generally, the latter method is more popular because of better control. For instance, ATRP has been applied recently as a controlled radical polymerization procedure that allows control over both molecular weight and architecture. One of the most popular multifunctional initiators is polyamidoamine (PAMAM) dendrimer (150,151) (see Dendrimers) and multihydroxyl-terminated PEG (152,153). The arm number of a star polymer is determined by the number of end groups in the core molecule. For PAMAM, the arm number increases proportionately with the addition generation. Three- and four-arm PEGs can be prepared by anionic polymerization of ethylene oxide initiated with potassium alkoxides of trimethylolpropane and pentaerythritol, respectively (154). Now, multihydroxyl-terminated PEGs with a controlled arm number and molecular weight per arm have been commercialized by Shearwater, Inc. (Huntsville, AL, USA). In most cases for star polymers, PEG not only plays the role as an initiator but is also the hydrophilic part of the polymeric system. Other initiators with multiple active groups were reported, including pentaerythritol (148) and 1,2,3,4,6-penta-*O*-isobutyryl bromide-α-D-glucose (155). Johnson and Fraser (156) prepared poly(lactic acid) and poly(acrylic acid) star polymers with luminescent ruthenium tris(bipyridine) centers (Scheme 19) to couple drug delivery and imaging functionality. Kovář *et al.* (157) also presented an interesting star structure polymer composed of HPMA copolymer–doxorubicin conjugates and targeting B1 monoclonal antibodies (Scheme 20). This is a more homogeneous and better characterized polymer than the classic hyperbranched antibody-targeted conjugates. Furthermore, they revealed that the star structure of the targeted conjugate has a remarkably higher antitumor effect than the classic structure, which may result from its higher cellular internalization rate and longer blood-elimination profile.

Compared with linear block polymer or polymer conjugation, research on star polymers as drug vectors seems rather limited so far. It has been shown that star-shaped polymers exhibit a smaller hydrodynamic radius and lower

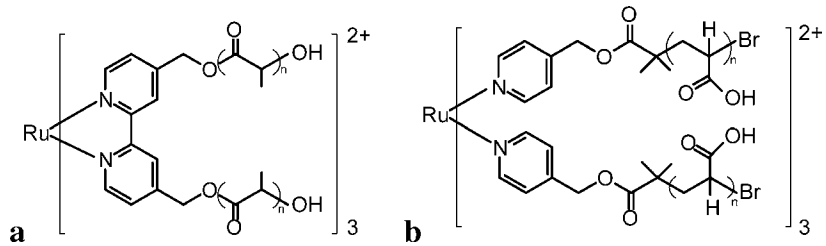

Scheme 19. (a) Poly(lactic acid) and (b) poly(acrylic acid) star polymers with luminescent ruthenium tris(bipyridine) centers.

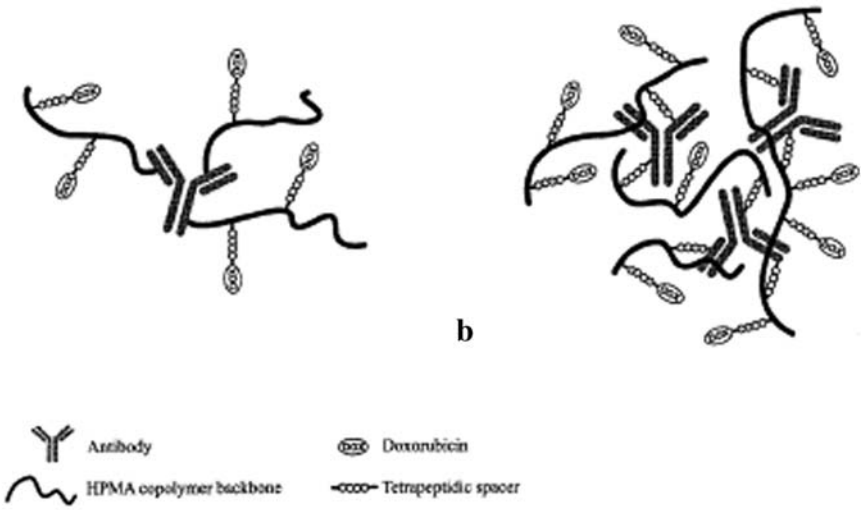

Scheme 20. (a) Antibody-targeted HPMA copolymer-bound doxorubicin conjugate and (b) the star structure polymer (157).

solution viscosity when compared to linear polymers of the same molecular weight and composition. The smaller hydrodynamic radius of PEG is important for complete renal excretion after acting. The structure of the star polymer makes it feasible to using PEG with higher molecular weights; thus, the system would be improved at controlling the hydrophilic/hydrophobic balance and core protection. However, the most significant point for star polymer-based unimolecular micelles is its higher stability compared with micelles formed from amphiphilic molecules because these unimolecular micelles contain covalently fixed branching points. It has been noticed that drug loading in the micelle can be obtained, but it is controlled by the dimension of hydrophobic core. Liu *et al.* (158) developed a three-arm star polymer composed of mucic acid substituted with fatty acid as a lipophilic inner block and PEG as the hydrophilic outer block. It could encapsulate a hydrophobic model drug in aqueous media, but because of structural constraints, only one or two drug molecules could be encapsulated inside each micelle. When using a dendrimer as the drug-loaded core, it was also demonstrated that micelles with a larger dendrimer core had higher encapsulation ability than those with smaller cores (159,160). To promote drug loading, lipophilic PCL inner blocks were linked to PAMAM dendrimer (Scheme 21) (151). An increased loading capacity of up to 22% (w/w) achieved with etoposide, a hydrophobic anticancer drug, was attributed to the enlarged core volume. Recently, charged star polymers have also been developed for gene delivery. Georgiou *et al.* (149) synthesized nanoscopic cationic methacrylate star homopolymers with varying degrees of polymerization of the arms from 10 to 100 using the arm-first method and evaluated the effect of polymer architecture on gene transfection. It was found that the p*K*'s of all star polymers were calculated to be between 6.7 and 7.0, independent of the arm DP. In contrast, the hydrodynamic diameters of the star polymers strongly depended upon the DP of the arms. All of star polymers were evaluated for their ability to transfect human cervical HeLa cancer cells with plasmid pRLSV40 modified with enhanced green fluorescent protein as a reporter gene. Results showed that as the DP of the arms of the DMAEMA star homopolymers increased from 10 to 100, the overall transfection efficiency decreased.

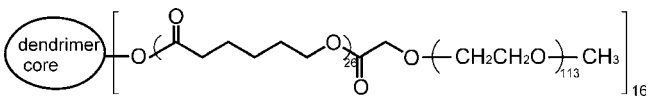

Scheme 21. Star polymer dendrimer–PCL–PEG.

Different from star polymers mentioned above, a series of star copolymers composed of a central hydrophilic PEG segment and temperature-responsive PNIPAAm terminal segments with arm numbers of 2, 4, and 8 have been prepared (152). Such polymers did not form micelles in aqueous media below the LCST of PNIPAAm because both blocks are hydrophilic; instead, they exhibited a reversible sol–gel transition process via a physical cross-linking mechanism upon warming to body temperature. Their structures and properties relationship were examined in detail. Comparison of the rheological results for the two-, four-, and eight-arm structures showed that polymers with four-arm structure formed gel in the highest strength. These materials look promising for *in situ* gelation applications such as injectable drug delivery and tissue engineering scaffolds. Star-shaped poly(ether-ester) block copolymers with the number of arms ranging from three to eight have also been studied systemically where PEG acted as the inner hydrophilic block and PLA or PCL as the outer hydrophobic block (154). Such polymers cannot form micelles because the hydrophilic block is located in the interior of the star. Polypeptide-loaded microspheres were prepared using these star-shaped polymers, and their drug release profiles were investigated *in vitro*. Physical properties because of molecular architecture influenced the microsphere preparation and drug release. As the number of arms increased, drug release was found to increase correspondingly that resulted from accelerated degradation of the highly branched polymer.

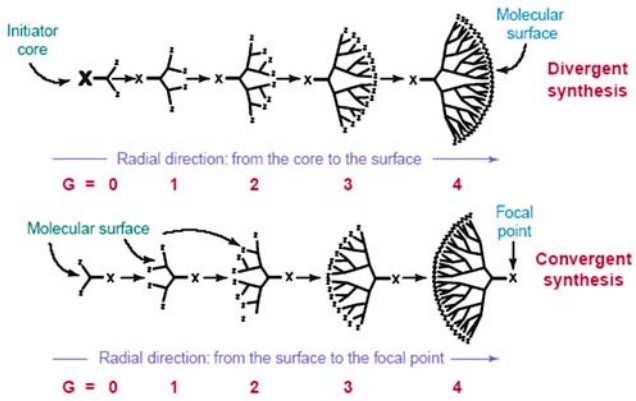

Scheme 22. Two principle synthetic methods for constructing dendrimer (172).

DENDRIMERS

Dendrimers represent a relatively new class of macromolecules having a unique three-dimensional structure in which a series of layered branches regularly extend from a central core (161,162). The term "dendrimer" is derived from the Greek words "dendra" for tree and "meros" for part. A typical dendrimer comprises three main structural components: a multifunctional central core, branched units, and surface groups. The repeated layers are called "generations."

Most dendrimer syntheses involve the repetition of a two-step reaction sequence, which consists of a generation growth step and an activation step. To obtain dendrimers without structural defects, both of these reactions must be clean and occur in high yields without any noticeable side reactions. Two general synthetic strategies have been developed to prepare dendrimers (Scheme 22): the divergent approach initiated by Tomalia *et al.* and Newkome *et al.* and the convergent approach by Hawker and Fréchet (163). Both synthetic approaches possess relative advantages and disadvantages, and the appropriate route depends mainly on the kind of monomer employed and the desired polymer structure. The most obvious difference between the two approaches is in the direction of dendrimer growth. In divergent synthesis, dendrimer growth starts from a polyfunctional core and expands outward with the stepwise addition of successive layers of building blocks. In contrast, in the convergent approach, dendrimer construction begins at what will eventually become the outer surface shell of an ideally branched macromolecule and proceeds inward by a step addition of branching monomers, followed by the final attachment of each branched dendritic subunit (or dendron) to a polyfunctional core. A comparison of the two methods suggests that the convergent approach affords better control over the ultimate dendritic architecture than the divergent

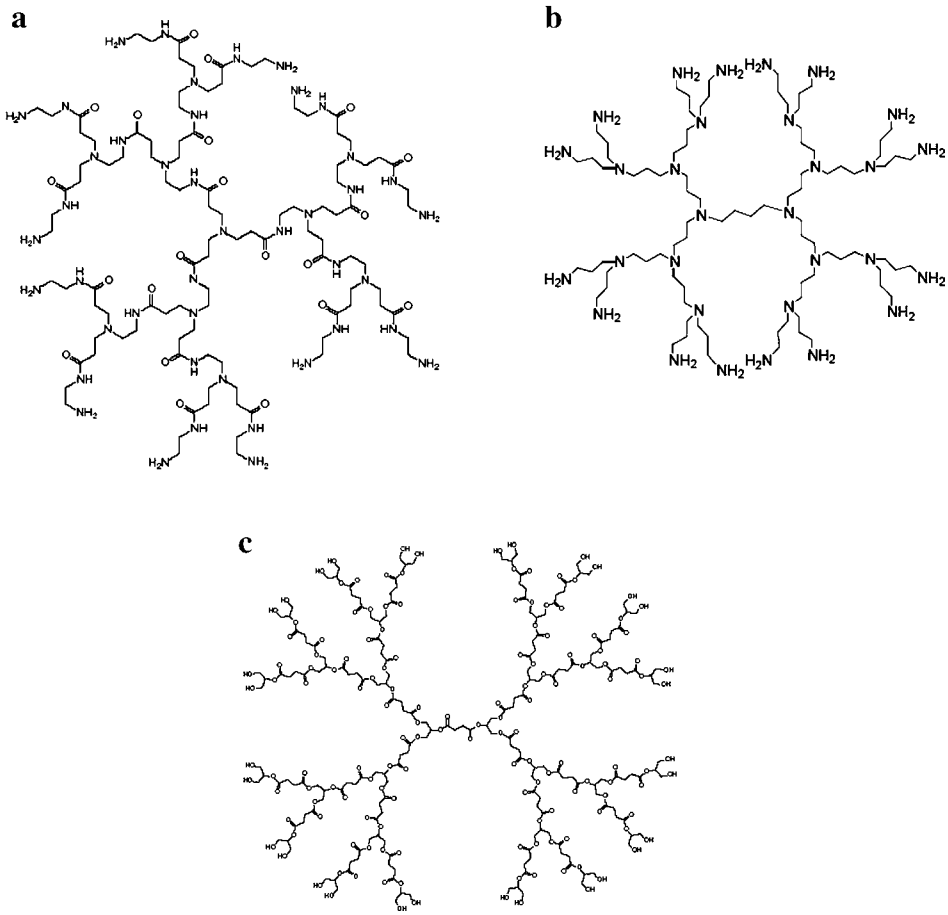

Scheme 23. (a) Polyamidoamine dendrimer; (b) polypropyleneimine (PPI) dendrimer; and (c) polyester dendrimer based on glycerol and succinic acid.

approach. On the other hand, the divergent approach has been shown to be suitable for larger-scale production of dendrimers. However, both methods involve stepwise processes that are tedious and time consuming. During the early stages, studies in dendrimer chemistry focused mainly on the development of synthesis methods, as well as the investigation of their physical and chemical properties. As a result, a large number of dendrimers with a variety of architectures have been prepared. Since the 1990s, numerous research groups have begun to explore various potential applications of dendrimers including drug delivery. The precise synthesis technique facilitates the emergence of several kinds of dendrimer backbones with good water solubility and biocompatibility.

PAMAM dendrimers (Scheme 23a) synthesized by divergent approach are the first complete dendrimer family to be commercialized. They have proven to be nonimmunogenic and have low mammalian toxicity, especially when their surface is modified with anionic or neutral groups such as carboxylic or hydroxylic moieties (150). Polypropyleneimine (PPI) dendrimer (Scheme 23b) is another commercialized material. Its shortcoming stems from the presence of multiple cationic amine groups, which relate to its high toxicity. Because biodegradation is always one of the crucial factors for biological materials, some biodegradable dendrimers have been designed to undergo metabolism. For example, peptide-based dendrimers, such as polylysine, have been developed as potential biomaterials (164). Polyester dendrimers incorporating monomers, such as glycerol, succinic acid, phenylalanine, and lactic acid, have been prepared by Grinstaff (165) (Scheme 23c), and their potential uses in tissue engineering have been demonstrated. These biodegradable dendrimers may provide numerous opportunities to deliver drugs via various parenteral routes. Given PEG's characteristics, it has been often introduced into the dendrimer molecules to obtain PEG dendritic analogs.

As described in several recent reviews, the application of dendrimers in the field of drug delivery has been explored ranging from anticancer, antiviral, antibacterial drugs and vaccines to gene and magnetic resonance imaging contrast agents. In addition, drug-contained dendrimer systems have been designed to achieve targeted injection, oral, ocular, and transdermal delivery (166–171). Compared to linear polymers, dendrimers exhibit unique architecture, which can provide several advantages for drug delivery applications. First, the internal cavity of the dendrimer provides a location for hydrophobic drug to achieve noncovalent encapsulation with the possibility of subsequent controlled release. Second, the controlled multivalency of dendrimers can be used to attach combination of drug molecules, targeting groups and solubilizing groups to the periphery of the dendrimers in a well-defined manner. Third, the more globular shape of dendrimers, rather than the random coil structure of most linear polymers, could affect their biological properties, and the low polydispersity of dendrimers should provide reproducible pharmacokinetic behavior. Lastly, unlike polymeric micelles, dendritic micelles are quite stable at any concentration because such unimolecular covalently bound micelles do not dissociate.

Dendrimer drug delivery offers a uniform and promising protocol for drug entrapment, conjugation, and controlled release. It is worth noting the relationship between dendrimer architecture and pharmacokinetics or drug bioavailability. Dendrimer architecture covers factors such as the chemical property and size of branched units, i.e., generation number (G), which always exerts the most critical influence on the quality of the resultant system, such as size, drug-loading capability, efficiency, and safety.

Based on its open and extending linkage mode of repeated units, the dimensional scale of dendrimers universally exhibits a simple dependence relationship on the generation number. PAMAM dendrimer is just a typical example to illustrate. The diameters of PAMAM spherical molecules are 40, 53, 67, and 80 Å, respectively, which is exactly proportional to generation numbers of 4, 5, 6, and 7 (172). When the dendrimer works as a host to physically entrap the guest drug, relatively high generation is expected to strengthen the interaction between the dendrimer and the drug, especially under conditions when hydrogen bonding or hydrophobic interactions drive the drug loading (155,173). Studies show that the generation will also affect drug release to a certain extent. For PAMAM dendrimer, core-tethered amplifications transform dendrimers from flexible scaffolding (G0–3) to semirigid container-type structures (G4–6). These container-type host structures exhibit guest-molecule permeability. In contrast, rigid surface-scaffolding structures (G7–10) manifest limited surface permeability, which consequently is supposed to sustain drug release (172). Bhadra *et al.* (174) prepared PPI dendrimer loaded with primaquine phosphate, an antimalarial drug, using an equilibrium dialysis method. There was an increase in drug entrapment by 5–15 times with increasing generation. Moreover, as expected, drug release is obviously retained by dendrimers with a large generation because with increased generations, the structures become more compact and peripherally closer. Similar results were reported with paclitaxel-loaded polyglycerol dendrimers (155). In the second strategy of chemically conjugating drugs to dendrimers, the greater the generation, the larger the dendrimer size, which produces more end groups for the drug to bind. Moreover, drug release can be controlled by incorporating hydrolysis linkages between the drug and the dendrimer. Zhou *et al.* (175) have described the influence of generation on the amount of 5-fluorouracil (5FU) in 5FU-conjugated PAMAM dendrimers with different generations.

Several research groups have revealed that drug-loaded dendrimers can facilitate penetration into the cell and bypass drug efflux transporters, therefore increasing drug bioavail-

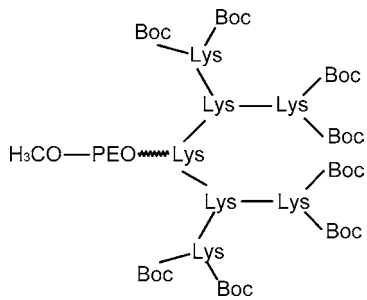

Scheme 24. Hydra-amphiphiles that consist of a dendrimer as the nonpolar component and a PEG chain as the polar component.

ability (176,177). In the boronated starburst dendrimer–monoclonal–antibody immunoconjugates system (178), the zero-generation starburst dendrimer with three terminal amino groups had the lowest hepatic and spleenic uptake of the injected dose of radioactivity at 72 h, with 1 and 0.01%, respectively. Higher-generation dendrimers (G2–4) have five times higher hepatic uptake than zero-generation dendrimers. Using an everted rat intestinal sac system, the effect of PAMAM dendrimer size on uptake and transport across adult rat intestine *in vitro* was investigated (179). The results showed the size or conformation sensitivity of the transport mechanism, indicating that a generation 5.5 dendrimer displayed higher tissue accumulation compared with that of either a generation 2.5 or 3.5 dendrimer. Patri *et al.* (180) concentrated on this in their review.

As Malik *et al.* (181) revealed, the biocompatibility or safety of dendrimers *in vivo* is dominated by its charge. In general, regardless of structure, cationic dendrimers were hemolytic and cytotoxic even at relatively low concentrations. Moreover, in the case of PAMAM dendrimers, hemolysis was generation-dependent, increasing with higher generations. Conversely, dendrimers with carboxylate-terminal groups were neither hemolytic nor did they cause cytotoxicity across a panel of cell lines studied *in vitro*.

Recently, a new series of architectures derived from dendrimer has been reported. Chapman *et al.* (182) presented hydra-amphiphiles that consist of a dendrimer as the nonpolar component and a PEG chain as the polar component (Scheme 24). The amphiphilic polymers described by Zhong and Eisenberg (183) can be regarded as the first approach toward PSt-dendrimer structures with variable polar head-group size. PPI dendrimers were used as the polar portion in amphiphilic block copolymers because of their good hydrophilicity and highly branched structure. van Hest *et al.* (184) reported on the synthesis and

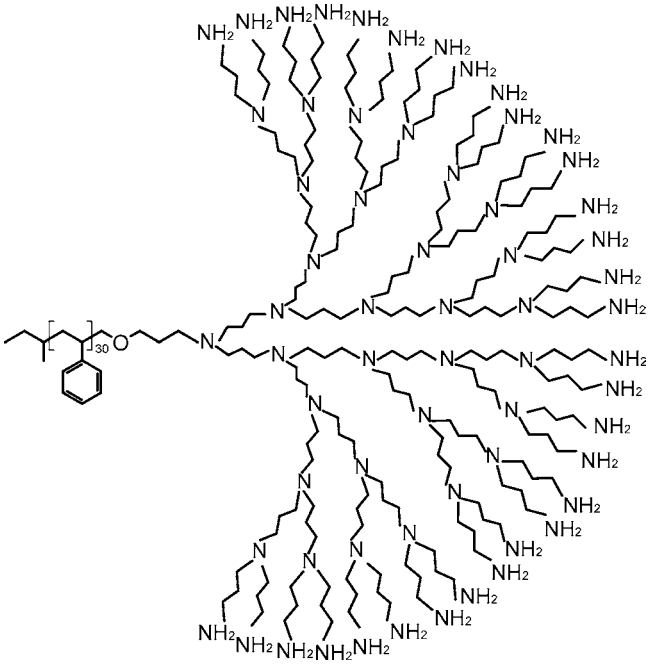

Scheme 25. Block copolymer with a polystyrene chain and a PPI dendrimer.

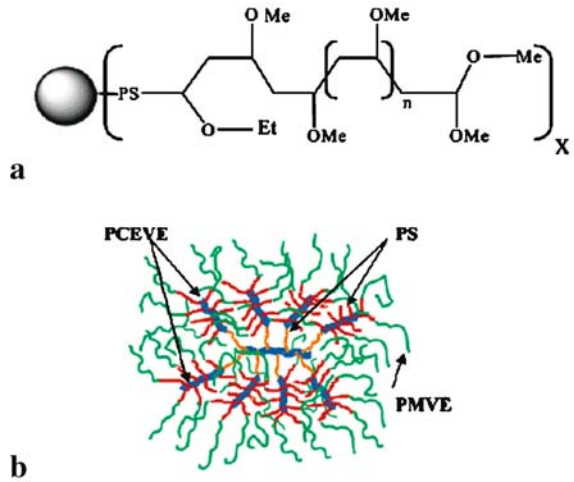

Scheme 26. Dendrigraft with a PSt core and PSt–*b*-poly(methyl vinyl ether) (PMVE) as external branches. PCEVE: poly(chloroethyl vinyl ether) (186).

characterization of a well-defined class of hybrid PSt-dendrimer block copolymers (Scheme 25) for which the head-group size varied by five different generations, from PSt-dendr-NH_2 up to PSt-dendr-$(NH_2)_{32}$. The results showed that in aqueous phases, PSt-dendr-$(NH_2)_{32}$ formed spherical micelles, PSt-dendr-$(NH_2)_{16}$ formed micellar rods, and PSt-dendr-$(NH_2)_8$ formed vesicular structures. Lower generations of this class of macromolecules show inverted micellar behavior.

Zhu *et al.* (185) prepared an asymmetric linear-dendritic block copolymer of polyether dendrimer and PNIPAm by an ATRP method. It was found that a thermosensitive phase transition took place at 37.5°C, whereas spherical aggregates of this block dendritic polymer simultaneously grew into larger entangled nanotubules. These unique temperature-sensitive supramolecular aggregates may be especially useful as intelligent capsules for drug delivery systems and as chemical sensors.

Schappacher *et al.* (186) constructed a water-soluble dendrigraft with a PSt core and PSt-*b*-poly(methyl vinyl ether) as external branches (Scheme 26). The dendrigrafts were observed by AFM and TEM to be egg-like or long cylindrical objects, which could self-organize intramolecularly into segregated subdomains, forming flowerlike or strings of flowerlike objects. In addition, the dendrigrafts in water showed an LCST above 30°C.

CONCLUSIONS

The ultimate goal for controlled drug release is to maximize therapeutic activity while minimizing the negative side effects of the drug. In this regard, versatile nanoscale delivery approaches based on novel biomaterials have already been established to seek the distinct advantages in drug treatment and diagnosis. Numerous efforts have rendered this point much clearer that nanotechnology utilized in the controlled drug systems does not simply imply the dimension reduction, but instead emphasizes significant functions related to the decreased size. The architecture–

property relationship is at the heart of this rational concept because the architecture of the polymer markedly influences not only the physicochemical properties of the polymer itself under the request of *in vivo* application, but it also influences various aspects of the drug itself, including drug-loading efficiency, drug release rate, biodistribution, and even interaction with specific tissues or cells *in vivo*. So far, several specific criteria of polymers have been addressed to fabricate novel drug delivery systems related to nanotechnology (Table I). Optimizing polymer architecture is an intelligent strategy to develop desired pharmaceutical products. However, the study experience on some relatively new drug carriers, such as dendrimer and polymersome, is still quite limited, and there are not enough experimental data to comprehensively understand the influence of these polymer architectures on the fate of drugs. Therefore, more extensive work is urgently required. In addition, some properties of drug delivery systems, such as yield and stability, which have to be considered during practical manufacture, also need further investigation from the view of polymer architecture. In a word, studies on polymer architecture would be beneficial to further elucidate the action mechanisms of drug delivery systems, and more importantly, it would also offer a valuable feedback to properly tune-make and optimize biopolymers of a new generation for high-quality drug products.

With the advances in polymer synthesis chemistry and technology, more defined, controlled, and biocompatible polymers are becoming available, and such polymers will contribute to new generations of biomimetic nanostructures and vehicles for carrying diagnostic and imaging agents, therapeutic drugs, prognostic reagents, and multiagents in the future. Thus, controlling polymer architecture will be one of the most crucial technologies for future drug delivery. The new polymers and nanocarriers definitely require extensive consideration of toxicological and immunological issues, which are often ignored during the research phase.

ACKNOWLEDGMENTS

This review work is partially supported by NIH CA101850, and Dr. L. Y. Qiu is supported by the State Scholarship Fund of China (2004833013).

REFERENCES

1. J. Folkman and D. M. Long. The use of silicone rubber as a carrier for prolonged drug therapy. *J. Surg. Res.* **4**:139–142 (1964).
2. A. Rösler, G. W. M. Vandermeulen, and H. A. Klok. Advanced drug delivery devices via self-assembly of amphiphilic block copolymers. *Adv. Drug Deliv. Rev.* **53**:95–108 (2001).
3. I. Brigger, C. Dubernet, and P. Couvreur. Nanoparticles in cancer therapy and diagnosis. *Adv. Drug Deliv. Rev.* **54**:631–651 (2002).
4. J. Panyam and V. Labhasetwar. Biodegradable nanoparticles for drug and gene delivery to cells and tissue. *Adv. Drug Deliv. Rev.* **55**:329–347 (2003).
5. A. Lavasanifar, J. Samuel, and G. S. Kwon. Poly(ethylene oxide)-*block*-poly(L-amino acid) micelles for drug delivery. *Adv. Drug Deliv. Rev.* **54**:169–190 (2002).
6. T. Peng and Y.-L. Cheng. PNIPAAm and PMAA co-grafted porous PE membranes: living radical co-grafting mechanism and multi-stimuli responsive permeability. *Polymer* **42**:2091–2100 (2001).
7. K. Hoste, K. De Winne, and E. Schacht. Polymeric prodrugs. *Int. J. Pharm.* **277**:119–131 (2004).
8. M. G. McKee, S. Unal, G. L. Wilkes, and T. E. Long. Branched polyesters: recent advances in synthesis and performance. *Prog. Polym. Sci.* **30**:507–539 (2005).
9. H. Ringsdorf. Structure and properties of pharmacologically active polymers. *J. Polym. Sci. Symp.* **51**:135–153 (1975).
10. R. Duncan. Polymer–drug conjugates. In H. Budman, H. Calvert, and E. Rowinsky (eds.), *Handbook of Anticancer Drug Development*, Lippincott Williams and Wilkins, Baltimore, 2003, pp. 239–260.
11. T. Okana, N. Yui, M. Yokoyama, and R. Yoshida. *Advances in Polymeric Systems for Drug Delivery*, Gordon and Breach Science Publisher, Tokyo, 1994.
12. R. Duncan. N-(2-Hydroxypropyl) methacrylamide copolymer conjugate. In G. S. Kwon (ed.), *Drug and the Pharmaceutical Sciences. Volume 148. Polymeric Drug Delivery Systems*, Taylor & Francis Group, Boca Raton, 2005, pp. 1–92.
13. L. W. Seymour, Y. Miyamoto, H. Maeda, M. Brereton, J. Strohalm, K. Ulbrich, and R. Duncan. Influence of molecular weight on passive tumour accumulation of a soluble macromolecular drug carrier. *Eur. J. Cancer* **31A**:766–770 (1995).
14. H. Maeda. SMANCS and polymer-conjugated macromolecular drug: advantages in cancer chemotherapy. *Adv. Drug Deliv. Rev.* **6**:181–202 (1991).
15. S. Tsunoda, H. Kamada, Y. Yamamoto, T. Ishikawa, J. Matsui, K. Koizumi, Y. Kaneda, Y. Tsutsumi, Y. Ohsugi, T. Hirano, and T. Mayumi. Molecular design of polyvinylpyrrolidone-conjugated interleukin-6 for enhancement of *in vivo* thrombopoietic activity in mice. *J. Control. Release* **68**(3):335–341 (2000).
16. A. J. M. D'Souza, R. L. Schowen, and E. M. Topp. Polyvinylpyrrolidone–drug conjugate: synthesis and release mechanism. *J. Control. Release* **94**(1):91–100 (2004).
17. Y. Kaneda, Y. Tsutsumi, Y. Yoshioka, H. Kamada, Y. Yamamoto, H. Kodaira, S. Tsunoda, T. Okamoto, Y. Mukai, H. Shibata, S. Nakagawa, and T. Mayumi. The use of PVP as a polymeric carrier to improve the plasma half-life of drugs. *Biomaterials* **25**:3259–3266 (2004).
18. A. Kishida. A site-specific polymeric drug carrier for renal disease treatment. *Trends Pharmacol. Sci.* **24**(12):611–613 (2003).
19. H. Vermeersch and J. P. Remon. Immunogenicity of poly-D-lysine, a potential polymeric drug carrier. *J. Control. Release* **32**(3):225–229 (1994).
20. K. Hoste, E. Schacht, and L. Seymour. New derivatives of polyglutamic acid as drug carrier systems. *J. Control. Release* **65**:367–374 (2000).
21. E. J. F. Franssen, F. Moolenaar, D. De Zeeuw, and D. K. F. Meijer. Drug targeting to the kidney with low-molecular weight proteins. *Adv. Drug Deliv. Rev.* **14**:67–88 (1994).
22. S. Matsumoto, A. Yamamoto, Y. Takakura, M. Hashida, and H. Sezaki. Cellular interaction and *in vitro* antitumour activity of mitomycin C-dextran conjugate. *Cancer Res.* **46**:4463–4468 (1986).
23. A. Al-Shamkhani and R. Duncan. Synthesis, controlled release properties and antitumour activity of alginate–*cis*-aconityl–daunomycin conjugates. *Int. J. Pharm.* **122**(1–2):107–119 (1995).
24. Y. J. Son, J. S. Jang, Y. W. Cho, H. Chung, R. W. Park, I. C. Kwon, I. S. Kim, J. Y. Park, S. B. Seo, C. R. Park, and S. Y. Jeong. Biodistribution and anti-tumor efficacy of doxorubicin loaded glycol–chitosan nanoaggregates by EPR effect. *J. Control. Release* **91**(1–2):135–145 (2003).
25. D. H. W. Ho, C. Wang, J. Lin, N. Brown, R. A. Newman, and I. H. Krakoff. Polyethylene glycol–L-asparaginase and L-asparaginase studies in rabbits. *Drug Metab. Dispos.* **16**:27–29 (1988).
26. H. Tanaka, R. Satake-Ishakawa, M. Ishakawa, S. Matsuki, and K. Asano. Pharmacokinetics of recombined human granulocyte colony-stimulating factor conjugated to poly(ethylene glycol) in rats. *Cancer Res.* **51**:3710–3714 (1991).

27. R. Tomlinson, J. Heller, S. Brocchini, and R. Duncan. Polyacetal–doxorubicin conjugates designed for pH-dependent degradation. *Bioconjug. Chem.* **14**:1096–1106 (2003).
28. A. Nori and J. Kopeček. Intracellular targeting of polymer-bound drug drugs for cancer chemotherapy. *Adv. Drug Deliv. Rev.* **57**:609–636 (2005).
29. L. W. Seymour, R. Duncan, J. Strohalm, and J. Kopeček. Effect of molecular weight (.hivin.Mw) of *N*-(2-hydroxypropyl)methacrylamide copolymers on body distribution and rate of excretion after subcutaneous, intraperitoneal, and intravenous administration to rats. *J. Biomed. Mater. Res.* **21**:1341–1358 (1987).
30. K. Riebeseel, E. Biedermann, R. Löser, N. Breiter, R. Hanselmann, R. Mülhaupt, C. Unger, and F. Kratz. Polyethylene glycol conjugates of methotrexate varying in their molecular weight from MW 750 to MW 40000: synthesis, characterization, and structure–activity relationships *in vitro* and *in vivo*. *Bioconjug. Chem.* **13**:773–785 (2002).
31. F. M. Veronese, O. Schiavon, G. Pasut, R. Mendichi, L. Andersson, A. Tsirk, J. Ford, G. Wu, S. Kneller, J. Davies, and R. Duncan. PEG–doxorubicin conjugates: influence of polymer structure on drug release, *in vitro* cytotoxicity, biodistribution, and antitumor activity. *Bioconjug. Chem.* **16**(4):775–784 (2005).
32. Y. Yamamoto, Y. Tsutsumi, Y. Yoshioka, H. Kamada, K. Sato-Kamada, T. Okamoto, Y. Mukai, H. Shibata, S. Nakagawa, and T. Mayumi. Poly(vinylpyrrolidone-*co*-dimethyl maleic acid) as a novel renal targeting carrier. *J. Control. Release* **95**(2):229–237 (2004).
33. H. Kodaira, Y. Tsutsumi, Y. Yoshioka, H. Kamada, Y. Kaneda, Y. Yamamoto, S. Tsunoda, T. Okamoto, Y. Mukai, H. Shibata, S. Nakagawa, and T. Mayumi. The targeting of anionized polyvinylpyrrolidone to the renal system. *Biomaterials* **25**:4309–4315 (2004).
34. Y. Yoshioka, Y. Tsutsumi, Y. Mukai, H. Shibata, T. Okamoto, Y. Kaneda, S. Tsunoda, H. Kamada, K. Koizumi, Y. Yamamoto, Y. Mu, H. Kodaira, K. Sato-Kamada, S. Nakagawa, and T. Mayumi. Effective accumulation of poly(vinylpyrrolidone-*co*-vinyl laurate) into the spleen. *J. Biomed. Mater. Res. Part A* **70**(2):219–223 (2004).
35. H. Soyez, E. Schacht, and S. Vanderkerken. The crucial role of spacer groups in macromolecular prodrug design. *Adv. Drug Deliv. Rev.* **21**:81–106 (1996).
36. S. Sakuma, Z. R. Lu, P. Kopečková, and J. Kopeček. Biorecognizable HPMA copolymer–drug conjugates for colon-specific delivery of 9-aminocamptothecin. *J. Control. Release* **75**(3):365–379 (2001).
37. Z. R. Lu, J. G. Shiah, S. Sakuma, P. Kopečková, and J. Kopeček. Design of novel bioconjugates for targeted drug delivery. *J. Control. Release* **78**(1–3):165–173 (2002).
38. K. Ulbrich and V. Šubr. Polymeric anticancer drugs with pH-controlled activation. *Adv. Drug Deliv. Rev.* **56**:1023–1050 (2004).
39. W. C. Shen and H. J. P. Ryser. *cis*-Aconityl spacer between daunomycin and macromolecular carriers—a model of pH-sensitive linkage releasing drug from a lysosomotropic conjugate. *Biochem. Biophys. Res. Commun.* **102**:1048–1054 (1981).
40. W. M. Choi, P. Kopečková, T. Minko, and J. Kopeček. Synthesis of HPMA copolymer containing adriamycin bound via an acid-labile spacer and its activity toward human ovarian carcinoma cells. *J. Bioact. Compat. Polym.* **14**:447–456 (1999).
41. K. Ulbrich, T. Etrych, P. Chytil, M. Jelínková, and B. Říhová. HPMA copolymers with pH-controlled release of doxorubicin. *In vitro* cytotoxicity and *in vivo* antitumor activity. *J. Control. Release* **87**:33–47 (2003).
42. E. R. Gilles, A. P. Goodwin, and J. M. J. Frèchet. Acetals as pH-sensitive linkages for drug delivery. *Bioconjug. Chem.* **15**:1254–1263 (2004).
43. M. J. Vicent, R. Tomlinson, S. Brocchini, and R. Duncan. Polyacetal–diethylstilboestrol: a polymeric drug designed for pH-triggered activation. *J. Drug Target.* **12**(8):491–501 (2004).
44. S. Jaracz, J. Chen, L. V. Kuznetsova, and I. Ojima. Recent advances in tumor-targeting anticancer drug conjugates. *Bioorg. Med. Chem.* **13**(17):5043–5054 (2005).
45. M. Nishikawa. Development of cell-specific targeting systems for drugs and genes. *Biol. Pharm. Bull.* **28**(2):195–200 (2005).
46. N. Kumar, M. N. V. Ravikumar, and A. J. Domb. Biodegradable block copolymers. *Adv. Drug Deliv. Rev.* **53**:23–44 (2001).
47. Y. Bae and K. Kataoka. Polymer assemblies: intelligent block copolymer micelles for the programmed delivery of drugs and genes. In G. S. Kwon (ed.), *Drug and the Pharmaceutical Sciences. Volume 148. Polymeric Drug Delivery Systems*, Taylor & Francis Group, Boca Raton, 2005, pp. 491–532.
48. H. Bader, H. Ringsdorf, and B. Schmidt. Water soluble polymers in medicine. *Angew. Chem.* **123–124**:457–485 (1984).
49. M. K. Pratten, J. B. Lloyd, G. Horpel, and H. Ringsdorf. Micelle-forming block copolymers: pinocytosis by macrophages and interaction with model membranes. *Makromol. Chem.* **186**:725–733 (1985).
50. A. V. Kabanov, V. P. Chekhonin, V. Y. Alakhov, E. V. Batrakova, A. S. Lebedev, N. S. Melik-Nubarov, S. A. Arzhakov, A. V. Levashov, G. V. Morozov, E. S. Severin, and V. A. Kabanov. The neuroleptic activity of haloperidol increases after its solubilization in surfactant micelles: micelles as microcontainers for drug targeting. *FEBS Lett.* **258**:343–345 (1989).
51. M. Yokoyama, S. Inoue, K. Kataoka, N. Yui, and Y. Sakurai. Preparation of adriamycin-conjugated poly(ethylene glycol)–poly(aspartic acid) block copolymer. A new type of polymeric anticancer agent. *Makromol. Chem., Rapid. Commun.* **8**:431–435 (1987).
52. M. Yokoyama, S. Inoue, K. Kataoka, N. Yui, and Y. Sakurai. Molecular design for missile drug: synthesis of adriamycin conjugated with IgG using poly(ethylene glycol)–poly(aspartic acid) block copolymer as intermediate carrier. *Makromol. Chem.* **190**:2041–2054 (1989).
53. M. Yokoyama, A. Satoh, Y. Sakurai, T. Okano, Y. Matsumura, T. Kakizoe, and K. Kataoka. Incorporation of water-insoluble anti-cancer drug into polymeric micelles and control of their particle size. *J. Control. Release* **55**:219–229 (1998).
54. M. Yokoyama. Polymeric micelles for the targeting of hydrophobic drugs. In G. S. Kwon (ed.), *Drug and the Pharmaceutical Sciences. Volume 148. Polymeric Drug Delivery Systems*, Taylor & Francis Group, Boca Raton, 2005, pp. 533–575.
55. P. Ferruti, M. Penco, P. D'Addato, E. Ranucci, and R. Deghenghi. Synthesis and properties of novel block copolymers containing poly(lactic-glycolic acid) and poly(ethyleneglycol) segments. *Biomaterials* **16**:1423–1428 (1995).
56. R. T. Liggins and H. M. Burt. Polyether–polyester diblock copolymers for the preparation of paclitaxel loaded polymeric micelle formulations. *Adv. Drug Deliv. Rev.* **54**:191–202 (2002).
57. Y. I. Jeong, J. B. Cheon, S. H. Kim, J. W. Nah, Y. M. Lee, Y. K. Sung, T. Akaike, and C. S. Cho. Clonazepam release from core-shell type nanoparticles *in vitro*. *J. Control. Release* **51**(2–3): 169–178 (1998).
58. M. C. Woodle, C. M. Engbers, and S. Zalipsky. New amphipathic polymer-lipid conjugates forming long-circulating reticuloendothelial system-evading liposomes. *Bioconjug. Chem.* **4**:493–496 (1998).
59. V. P. Torchilin, T. S. Levchenko, K. R. Whiteman, A. A. Yaroslavov, A. M. Tsatsakis, A. K. Rizos, E. V. Mikhailova, and M. I. Shtilman. Amphiphilic poly-*N*-vinylpyrrolidones: synthesis, properties and liposome surface modification. *Biomaterials* **22**:3035–3044 (2001).
60. V. P. Torchilin. PEG-based micelles as carriers of contrast agents for different imaging modalities. *Adv. Drug Deliv. Rev.* **54**:235–252 (2002).
61. Y. Chang, J. D. Bender, M. V. B. Phelps, and H. R. Allcock. Synthesis and self-association behavior of biodegradable amphiphilic poly[bis(ethyl glycinat-*N*-yl)phosphazene]–poly(ethylene oxide) block copolymers. *Biomacromolecules* **3**:1364–1369 (2002).
62. Y. Chang, R. Prange, H. R. Allcock, S. C. Lee, and C. Kim. Amphiphilic poly[bis(trifluoroethoxy)phosphazene]–poly(ethylene oxide) block copolymers: synthesis and micellar characteristics. *Macromolecules* **35**:8556–8559 (2002).
63. H. R. Allcock, E. S. Powell, and Y. Chang. Synthesis and micellar behavior of amphiphilic polystyrene–poly [bis(methoxyethoxyethoxy)phosphazene] block copolymers. *Macromolecules* **37**:7163–7167 (2004).

64. Y. Chang, S. C. Lee, K. T. Kim, C. Kim, S. D. Reeves, and H. R. Allcock. Synthesis and micellar characterization of an amphiphilic diblock copolyphosphazene. *Macromolecules* **34**: 269–274 (2001).
65. S. Katayose and K. Kataoka. Water-soluble polyion complex associates of DNA and poly(ethylene glycol)–poly(L-lysine) block copolymer. *Bioconjug. Chem.* **8**:702–707 (1997).
66. T. Merdan, J. Callahan, H. Petersen, K. Kunath, U. Bakowsky, P. Kopećková, T. Kissel, and J. Kopećek. Pegylated polyethylenimine-Fab′ antibody fragment conjugates for targeted gene delivery to human ovarian carcinoma cells. *Bioconjug. Chem.* **14**:989–996 (2003).
67. K. Kataoka, A. Harada, D. Wakebayashi, and Y. Nagasaki. Polyion complex micelles with reactive aldehyde groups on their surface from plasmid DNA and end-functionalized charged block copolymers. *Macromolecules* **32**:6892–6894 (1999).
68. M. Yokoyama, T. Okano, Y. Sakurai, S. Suwa, and K. Kataoka. Introduction of cisplatin into polymeric micelle. *J. Control. Release* **39**:351–356 (1996).
69. N. Nishiyama, S. Okazaki, H. Cabral, M. Miyamoto, Y. Kato, Y. Sugiyama, K. Nishio, and K. Kataoka. Novel cisplatin-incorporated polymeric micelles can eradicate solid tumors in mice. *Cancer Res.* **63**:8977–8983 (2003).
70. V. S. Trubetskoy. Polymeric micelles as carriers of diagnostic agents. *Adv. Drug Deliv. Rev.* **37**:81–88 (1999).
71. A. Harada and K. Kataoka. Formation of stable and monodispersive polyion complex micelles in aqueous medium from poly(L-lysine) and poly(ethylene glycol)–poly(aspartic acid) block copolymer. *J. Macromol. Sci., Pure Appl. Chem.* **A34**:2119–2133 (1997).
72. A. Halperin. Rod-coil copolymers: their aggregation behavior. *Macromolecules* **23**:2724–2731 (1990).
73. L. F. Zhang and A. Eisenberg. Multiple morphologies and characteristics of "crew-cut" micelle-like aggregates of polystyrene–*b*-poly(acrylic acid) diblock copolymers in aqueous solutions. *J. Am. Chem. Soc.* **118**:3168–3181 (1996).
74. K. Yu and A. Eisenberg. Bilayer morphologies of self-assembled crew-cut aggregates of amphiphilic PS–*b*-PEO diblock copolymers in solution. *Macromolecules* **31**:3509–3518 (1998).
75. L. Zhang and A. Eisenberg. Multiple morphologies of "crew-cut" aggregates of polystyrene–*b*-poly(acrylic acid) block copolymers. *Science* **268**(5218):1728–1731 (1995).
76. L. Zhang, K. Yu, and A. Eisenberg. Ion-induced morphological changes in "crew-cut" aggregates of amphiphilic block copolymers. *Science* **272**(5269):1777–1779 (1996).
77. A. Lavasanifar, J. Samuel, and G. S. Kwon. Poly(ethylene oxide)-*block*-poly(L-amino acid) micelles for drug delivery. *Adv. Drug Deliv. Rev.* **54**:169–190 (2002).
78. K. Yasugi, Y. Nagasaki, M. Kato, and K. Kataoka. Preparation and characterization of polymer micelles from poly(ethylene glycol)–poly(D,L-lactide) block copolymers as potential drug carrier. *J. Control. Release* **62**:89–100 (1999).
79. J. Zastre, J. Jackson, M. Bajwa, R. Liggins, F. Iqbal, and H. Burt. Enhanced cellular accumulation of a *p*-glycoprotein substrate, rhodamine-123, by caco-2 cells using low molecular weight methoxypolyethylene glycol-*block*-polycaprolactone diblock copolymers. *Eur. J. Pharm. Biopharm.* **54**(3):299–309 (2002).
80. V. P. Torchilin, M. I. Shtilman, V. S. Trubetskoy, K. R. Whiteman, and A. M. Milsten. Amphiphilic vinyl polymers effectively prolong liposome circulation time *in vivo*. *Biochem. Biophys. Acta* **1195**:181–184 (1994).
81. G. H. V. Domeselaar, G. S. Kwon, L. C. Andrew, and D. S. Wishart. Application of solid phase peptide synthesis to engineering PEO-peptide block copolymers for drug delivery. *Colloids Surf., B Biointerfaces* **30**:323–334 (2003).
82. A. N. Lukyanov and V. P. Torchilin. Micelles from lipid derivatives of water-soluble polymers as delivery systems for poorly soluble drugs. *Adv. Drug Deliv. Rev.* **56**:1273–1289 (2004).
83. A. Harada, H. Togawa, and K. Kataoka. Physicochemical properties and nuclease resistance of antisense-oligonucleotides entrapped in the core of polyion complex micelles composed of poly(ethylene glycol)–poly(L-lysine) block copolymers. *Eur. J. Pharm. Sci.* **13**:35–42 (2001).
84. S. Katayose and K. Kataoka. Remarkable increase in nuclease resistance of plasmid DNA through supramolecular assembly with poly(ethylene glycol)–poly(L-lysine) block copolymer. *J. Pharm. Sci.* **87**:160–163 (1998).
85. M. Crothers, Z. Y. Zhou, N. M. P. S. Ricardo, Z. Yang, P. Taboada, C. Chaibundit, D. Attwood, and C. Booth. Solubilisation in aqueous micellar solutions of block copoly(oxyalkylene)s. *Int. J. Pharm.* **293**(1–2):91–100 (2005).
86. X. Zhang, J. K. Jackson, and H. M. Burt. Development of amphiphilic diblock copolymers as micellar carriers of taxol. *Int. J. Pharm.* **132**:195–206 (1996).
87. S. A. Hagan, A. G. Coombes, M. C. Garnett, M. C. Davies, L. Illum, and S. S. Davis. Polylactide–poly(ethylene glycol) copolymers as drug delivery systems. 1. Characterization of water dispersible micelle forming systems. *Langmuir* **12**:2153–2161 (1996).
88. T. Govender, T. Riley, T. Ehtezazi, M. C. Garnett, S. Stolnik, L. Illum, and S. S. Davis. Defining the drug incorporation properties of PLA–PEG nanoparticles. *Int. J. Pharm.* **199**:95–110 (2000).
89. A. N. Lukyanov, Z. Gao, and V. P. Torchilin. Micelles from polyethylene glycol/phosphatidylethanolamine conjugates for tumor drug delivery. *J. Control. Release* **91**:97–102 (2003).
90. A. N. Lukyanov, Z. Gao, L. Mazzola, and V. P. Torchilin. Polyethylene glycol-diacyllipid micelles demonstrate increased accumulation in subcutaneous tumors in mice. *Pharm. Res.* **19**:1424–1429 (2002).
91. Y. Kakizawa and K. Kataoka. Block copolymer micelles for delivery of gene and related compounds. *Adv. Drug Deliv. Rev.* **54**:203–222 (2002).
92. A. Agarwal, R. Unfer, and S. K. Mallapragada. Novel cationic pentablock copolymers as non-viral vectors for gene therapy. *J. Control. Release* **103**:245–258 (2005).
93. C. P. Leamon, D. Weigl, and R. W. Hendren. Folate copolymer-mediated transfection of cultured cells. *Bioconjug. Chem.* **10**:947–957 (1999).
94. Y. Teng, M. E. Morrison, P. Munk, and S. E. Webber. Release kinetics studies of aromatic molecules into water from block copolymer micelles. *Macromolecules* **31**:3578–3587 (1998).
95. F. Ahmed and D. E. Discher. Self-porating polymersomes of PEG–PLA and PEG–PCL: hydrolysis-triggered controlled release vesicles. *J. Control. Release* **96**(1):37–53 (2004).
96. S. K. Han, K. Na, and Y. H. Bae. Sulfonamide based pH-sensitive polymeric micelles: physicochemical characteristics and pH-dependent aggregation. *Colloids Surf., A Physicochem. Eng. Asp.* **214**:49–59 (2003).
97. E. S. Lee, H. J. Shin, K. Na, and Y. H. Bae. Poly(L-histidine)–PEG block copolymer micelles and pH-induced destabilization. *J. Control. Release* **90**:363–374 (2003).
98. F. Kohori, K. Sakai, T. Aoyagi, M. Yokoyama, Y. Sakurai, and T. Okano. Preparation and characterization of thermally responsive block copolymer micelles comprising poly(*N*-isopropylacrylamide-*b*-DL-lactide). *J. Control. Release* **55**:87–98 (1998).
99. J. E. Chung, M. Yokoyama, M. Yamato, T. Aoyagi, Y. Sakurai, and T. Okano. Thermo-responsive drug delivery from polymeric micelles constructed using block copolymer of poly(*N*-isopropylacrylamide) and poly(butylmethacrylate). *J. Control. Release* **62**:115–127 (1999).
100. F. Kohori, M. Yokoyama, K. Sakai, and T. Okano. Process design for efficient and controlled drug incorporation into polymeric micelle carrier systems. *J. Control. Release* **78**:155–163 (2002).
101. Y. Kakizawa, A. Harada, and K. Kataoka. Environment-sensitive stabilization of core-shell structured polyion complex micelle by reversible cross-linking of the core through disulfide bond. *J. Am. Chem. Soc.* **121**:11247–11248 (1999).
102. Y. Kakizawa, A. Harada, and K. Kataoka. Glutathione-sensitive stabilization of block copolymer micelles composed of antisense DNA and thiolated poly(ethylene glycol)-*block*-poly(L-lysine): a potential carrier for systemic delivery of antisense DNA. *Biomacromolecules* **2**:491–497 (2001).
103. N. Nishiyama and K. Kataoka. Preparation and characterization of size-controlled polymeric micelle containing *cis*-dichloro-

diammineplatinum(II) in the core. *J. Control. Release* **74**(1–3): 83–94 (2001).
104. J. J. Yuan, Z. S. Xu, S. Y. Cheng, L. X. Feng. The aggregation of polystyrene–*b*-poly(ethylene oxide)–*b*-polystyrene triblock copolymers in aqueous solution. *Eur. Polym. J.* **38**:1537–1546 (2002).
105. J. J. Yuan, Y. S. Li, X. Q. Li, S. Y. Cheng, L. Jiang, L. X. Feng, and Z. Q. Fan. The "crew-cut" aggregates of polystyrene–*b*-poly(ethylene oxide)–*b*-polystyrene triblock copolymers in aqueous media. *Eur. Polym. J.* **39**(4):767–776 (2003).
106. Y. Hu, L. Y. Zhang, Y. Cao, H. X. Ge, X. Q. Jiang, and C. Z. Yang. Degradation behavior of poly(ε-caprolactone)–*b*-poly (ethylene glycol)–*b*-poly(ε-caprolactone) micelles in aqueous solution. *Biomacromolecules* **5**:1756–1762 (2004).
107. B. Jeong, S. W. Kim, and Y. H. Bae. Thermosensitive sol–gel reversible hydrogels. *Adv. Drug Deliv. Rev.* **54**:37–51 (2002).
108. M. J. Hwang, J. M. Suh, Y. H. Bae, S. W. Kim, and B. Jeong. Caprolactonic poloxamer analog: PEG–PCL–PEG. *Biomacromolecules* **6**(2):885–890 (2005).
109. H. Kukula, H. Schlaad, M. Antonietti, and S. Förster. The formation of polymer vesicles or "peptosomes" by polybutadiene-*block*-poly(L-glutamate)s in dilute aqueous solution. *J. Am. Chem. Soc.* **124**(8):1658–1663 (2002).
110. F. Najafi and M. N. Sarbolouki. Biodegradable micelles/polymersomes from fumaric/sebacic acids and poly(ethylene glycol). *Biomaterials* **24**:1175–1182 (2003).
111. A. Napoli, M. J. Boerakker, N. Tirelli, R. J. M. Nolte, N. A. J. M. Sommerdijk, and J. A. Hubbell. Glucose-oxidase based self-destructing polymeric vesicles. *Langmuir* **20**(9):3487–3491 (2004).
112. A. Taubert, A. Napoli, and W. Meier. Self-assembly of reactive amphiphilic block copolymers as mimetics for biological membranes. *Curr. Opin. Chem. Biol.* **8**(6):598–603 (2004).
113. B. M. Discher, H. Bermudez, D. A. Hammer, D. E. Discher, Y.-Y. Won, and F. S. Bates. Cross-linked polymersome membranes: vesicles with broadly adjus properties. *J. Phys. Chem., B* **106**:2848–2854 (2002).
114. F. Ahmed and D. E. Discher. Self-porating polymersomes of PEG–PLA and PEG–PCL: hydrolysis-triggered controlled release vesicles. *J. Control. Release* **96**:37–53 (2004).
115. A. Napoli, N. Tirelli, E. Wehrli, and J. A. Hubbell. Lyotropic behavior in water of amphiphilic ABA triblock copolymers based on poly(propylene sulfide) and poly(ethylene glycol). *Langmuir* **28**:8324–8329 (2002).
116. A. K. Brannan and F. S. Bates. ABCA tetrablock copolymer vesicles. *Macromolecules* **37**:8816–8819 (2004).
117. Y. S. Yu and A. Eisenberg. Control of morphology through polymer–solvent interactions in crew-cut aggregates of amphiphilic block copolymers. *J. Am. Chem. Soc.* **119**:8383–8384 (1997).
118. J. Grumelard, A. Taubert, and W. Meier. Soft nanotubes from amphiphilic ABA triblock macromonomers. *Chem. Commun.* **13**:1462–1463 (2004).
119. F. Ahmed, A. Hategan, D. E. Discher, and B. M. Discher. Block copolymer assemblies with cross-link stabilization: from single-component monolayers to bilayer blends with PEO–PLA. *Langmuir* **19**:6505–6511 (2003).
120. A. T. Nikova, V. D. Gordon, G. Cristobal, M. R. Talingting, D. C. Bell, C. Evans, M. Joanicot, J. A. Zasadzinski, and D. A. Weitz. Swollen vesicles and multiple emulsions from block copolymers. *Macromolecules* **37**:2215–2218 (2004).
121. P. J. Photos, L. Bacakova, B. Discher, F. S. Bates, and D. E. Discher. Polymer vesicles *in vivo*: correlations with PEG molecular weight. *J. Control. Release* **90**:323–334 (2003).
122. D. R. Arifin and A. F. Palmer. Polymersome encapsulated hemoglobin: a novel type of oxygen carrier. *Biomacromolecules* **6**:2172–2181 (2005).
123. B. M. Discher, Y.-Y. Won, D. S. Ege, J.C.-M. Lee, F. S. Bates, D. E. Discher, and D. A. Hammer. Polymersomes: tough vesicles made from diblock copolymers. *Science* **284**(14): 1143–1146 (1999).
124. D. M. Vriezema, A. Kros, R. De Gelder, J. J. L. M. Cornelissen, A. E. Rowan, R. J. M. Nolte. Electroformed giant vesicles from thiophene-containing rod-coil diblock copolymers. *Macromolecules* **37**:4736–4739 (1999).
125. J. J. Lin, J. A. Silas, H. Bermudez, V. T. Milam, F. S. Bates, and D. A. and Hammer. The effect of polymer chain length and surface density on the adhesiveness of functionalized polymersomes. *Langmuir* **20**:5493–5500 (2004).
126. F. H. Meng, C. Hiemstra, G. H. M. Engbers, and J. Feijen. Biodegradable polymersomes. *Macromolecules* **36**:3004–3006 (2003).
127. B. M. Discher, D. A. Hammer, F. S. Bates, and D. E. Discher. Polymer vesicles in various media. *Curr. Opin. Colloid Interface Sci.* **5**:125–131 (2000).
128. H. Petersen, P. M. Fechner, D. Fischer, and T. Kissel. Synthesis, characterization and biocompatibility of polyethylenimine-*graft*-poly(ethylene glycol) block copolymers. *Macromolecules* **35**:6867–6874 (2002).
129. X. T. Shuai, T. Merdan, F. Unger, M. Wittmar, and T. Kissel. Novel biodegradable ternary copolymers hy-PEI–*g*-PCL–*b*-PEG: synthesis, characterization, and potential as efficient nonviral gene delivery vectors. *Macromolecules* **36**:5751–5759 (2003).
130. H. Y. Tian, C. Deng, H. Lin, J. R. Sun, M. X. Deng, X. S. Chen, and X. B. Jing. Biodegradable cationic PEG–PEI–PBLG hyperbranched block copolymer: synthesis and micelle characterization. *Biomaterials* **26**:4209–4217 (2005).
131. L. Tian, L. Yam, N. Zhou, H. Tat, and K. E. Uhrich. Amphiphilic scorpion-like macromolecules: design, synthesis, and characterization. *Macromolecules* **37**:538–543 (2004).
132. J. Djordjevic, M. Barch, and K. E. Uhrich. Polymeric micelles based on amphiphilic scorpion-like macromolecules: novel carriers for water-insoluble drugs. *Pharm. Res.* **22**(1):24–32 (2005).
133. L. Frauchiger, H. Shirota, K. E. Uhrich, and E. W. Castner Jr. Dynamic fluorescence probing of the local environments within amphiphilic starlike macromolecules. *J. Phys. Chem., B* **106**:7463–7468 (2002).
134. J. Djordjevic, B. Michniak, and K. E. Uhrich. Amphiphilic star-like macromolecules as novel carriers for topical delivery of nonsteroidal anti-inflammatory drugs. *AAPS PharmSci* **5**(4): (2003).
135. H. Q. Xie and D. Xie. Molecular design, synthesis and properties of block and graft copolymers containing polyoxyethylene segments. *Prog. Polym. Sci.* **24**:275–313 (1999).
136. Y. X. Li, J. Nothnagel, and T. Kissel. Biodegradable brush like graft polymers from poly(D,L-lactide) or poly(D,L-lactide-*co*-glycolide) and charge-modified, hydrophilic dextrans as backbone-synthesis, characterization and *in vitro* degradation properties. *Polymer* **38**(25):6197–6206 (1997).
137. K. Ito, H. Tsuchinda, T. Kitano, E. Yanada, and T. Matsumoto. Reactivity of poly (ethylene oxide) macromonomers in radical copolymerization. *Polym. J.* **17**:827–839 (1985).
138. F. Candau, F. Afchar, F. Taromi, and P. Rempp. Synthesis and characterization of polystyrene–poly(ethylene oxide) graft copolymers. *Polymer* **18**:1253–1257 (1977).
139. N. Bhattarai, H. R. Ramay, J. Gunn, F. A. Matsen, and M. Q. Zhang. PEG-grafted chitosan as an injec thermosensitive hydrogel for sustained protein release. *J. Control. Release* **103**(3):609–624 (2005).
140. H. K. Ju, S. Y. Kim, and Y. M. Lee. pH-temperature-responsive behaviors of semi-IPN and comb-type graft hydrogels composed of alginate and poly(*N*-isopropylacrylamide). *Polymer* **42**(16):6851–6857 (2001).
141. B. H. Lee, Y. M. Lee, Y. S. Sohn, and S.-C. Song. A thermosensitive poly(organophosphazene) gel. *Macromolecules* **35**:3876–3879 (2002).
142. B. H. Lee and S.-C. Song. Synthesis and characterization of biodegradable thermosensitive poly(organophosphazene) gels. *Macromolecules* **37**:4533–4537 (2004).
143. J. Y. Chang, P. J. Park, and M. J. Han. Synthesis of poly(4-methylphenoxy-phosphazene)-*graft*-poly(2-methyl-2-oxazoline) copolymers and their micelle formation in water. *Macromolecules* **33**:321–325 (2000).
144. J. X. Zhang, L. Y. Qiu, K. J. Zhu, and Y. Jin. Thermosensitive micelles self-assembled by novel *N*-isopropylacrylamide oligomer grafted polyphosphazene. *Macromol. Rapid Commun.* **25**:1563–1567 (2004).
145. J. X. Zhang, L. Y. Qiu, K. J. Zhu, and Y. Jin. Physicochemical characterization of polymeric micelles constructed from novel amphiphilic polyphosphazene with poly(*N*-isopropylacryl amide) and ethyl 4-aminobenzoate as side groups. *Colloids Surf., B Biointerfaces* **43**(3–4):123–270 (2005).

146. J. X. Zhang, L. Y. Qiu, K. J. Zhu, and Y. Jin. Thermosensitive self-assembly behaviors of novel amphiphilic polyphosphazenes. *Chin. Sci. Bull.* **50**(11):1–3 (2005).
147. J. X. Zhang, L. Y. Qiu, and K. J. Zhu. Engineering visible drug carriers based on biodegradable polyphosphazene. In *32nd Annual Meeting & Exposition of the Controlled Release Society*, Miami, 2005.
148. M.-C. Jones, M. Ranger, and J.-C. Leroux. pH-sensitive unimolecular polymeric micelles: synthesis of a novel drug carrier. *Bioconjug. Chem.* **14**:774–781 (2003).
149. T. K. Georgiou, M. Vamvakaki, C. S. Patrickios, E. N. Yamasaki, and L. A. Phylactou. Nanoscopic cationic methacrylate star homopolymers: synthesis by group transfer polymerization, characterization and evaluation as transfection reagents. *Biomacromolecules* **5**:2221–2229 (2004).
150. Q. Cai, Y. L. Zhao, J. Z. Bei, F. Xi, and S. G. Wang. Synthesis and properties of star-shaped polylactide attached to poly (amidoamine) dendrimer. *Biomacromolecules* **4**:828–834 (2003).
151. F. Wang, T. K. Bronich, A. V. Kabanov, R. D. Rauh, and J. Roovers. Synthesis and evaluation of a star amphiphilic block copolymer from poly(ε-caprolactone) and poly(ethylene glycol) as a potential drug delivery carrier. *Bioconjug. Chem.* **16**:397–405 (2005).
152. H. H. Lin and Y. L. Cheng. *In situ* thermoreversible gelation of block and star copolymers of poly(ethylene glycol) and poly(*N*-isopropylacrylamide) of varying architectures. *Macromolecules* **34**:3710–3715 (2001).
153. M. A. R. Meier, J.-F. Gohy, C.-A. Fustin, and U. S. Schubert. Combinatorial synthesis of star-shaped block copolymers: host–guest chemistry of unimolecular reversed micelles. *J. Am. Chem. Soc.* **126**:11517–11521 (2004).
154. Y. K. Choi, Y. H. Bae, and S. W. Kim. Star-shaped poly(ether-ester) block copolymers: synthesis, characterization, and their physical properties. *Macromolecules* **31**:8766–8774 (1998).
155. T. Ooya, J. Lee, and K. Park. Effects of ethylene glycol-based graft, star-shaped, and dendritic polymers on solubilization and controlled release of paclitaxel. *J. Control. Release* **93**:121–127 (2003).
156. R. M. Johnson and C. L. Fraser. Metalloinitiation routes to biocompatible poly(lactic acid) and poly(acrylic acid) stars with luminescent ruthenium tris(bipyridine) cores. *Biomacromolecules* **5**:580–588 (2004).
157. M. Kovář, J. Strohalm, T. Etrych, K. Ulbrich, and B. Říhová. Star structure of antibody-targeted HPMA copolymer-bound doxorubicin: a novel type of polymeric conjugate for targeted drug delivery with potent antitumor effect. *Bioconjug. Chem.* **13**:206–215 (2002).
158. H. Liu, A. Jiang, J. Guo, and K. E. Uhrich. Unimolecular micelles: synthesis and characterization of amphiphilic polymer systems. *J. Polym. Sci., A, Polym. Chem.* **37**:703–711 (1999).
159. M. Liu, K. Kono, and J. M. J. Fréchet. Water-soluble dendritic unimolecular micelles: their potential as drug delivery agents. *J. Control. Release* **65**:121–131 (2000).
160. C. Kojima, K. Kono, K. Maruyama, and T. Takagishi. Synthesis of polyamidoamine dendrimers having poly(ethylene glycol) grafts and their ability to encapsulate anticancer drugs. *Bioconjug. Chem.* **11**:910–917 (2000).
161. F. Aulenta, W. Hayes, and S. Rannard. Dendrimers: a new class of nanoscopic containers and delivery devices. *Eur. Polym. J.* **39**:1741–1771 (2003).
162. E. R. Gillies and J. M. J. Fréchet. Dendrimers and dendritic polymers in drug delivery. *DDT* **10**(1):35–43 (2005).
163. C. J. Hawker and J. M. J. Fréchet. Preparation of polymers with controlled molecular architecture. A new convergent approach to dendritic macromolecules. *J. Am. Chem. Soc.* **112**:7638–7647 (1990).
164. K. Sadler and J. P. Tam. Peptide dendrimers: applications and synthesis. *Rev. Mol. Biotech.* **90**(3–4):195–229 (2002).
165. M. W. Grinstaff. Biodendrimers; new polymeric biomaterials for tissue engineering. *Chemistry* **8**:2839–2846 (2002).
166. R. Wiwattanapatapee, L. Lomlim, and K. Saramunee. Dendrimers conjugates for colonic delivery of 5-aminosalicylic acid. *J. Control. Release* **88**(1):1–9 (2003).
167. T. F. Vandamme and L. Brobeck. Poly(amidoamine) dendrimers as ophthalmic vehicles for ocular delivery of pilocarpine nitrate and tropicamide. *J. Control. Release* **102**(1):23–38 (2005).
168. A. D'Emanuele, R. Jevprasesphant, J. Penny, and D. Attwood. The use of a dendrimer-propranolol prodrug to bypass efflux transporters and enhance oral bioavailability. *J. Control. Release* **95**(3):447–453 (2004).
169. A. S. Chauhan, S. Sridevi, K. B. Chalasani, A. K. Jain, S. K. Jain, N. K. Jain, and P. V. Diwan. Dendrimer-mediated transdermal delivery: enhanced bioavailability of indomethacin. *J. Control. Release* **90**(3):335–343 (2003).
170. Z. X. Wang, Y. Itoh, Y. Hosaka, I. Kobayashi, Y. Nakano, I. Maeda, F. Umeda, J. Yamakawa, M. Kawase, and K. Yag. Novel transdermal drug delivery system with polyhydroxyalkanoate and starburst polyamidoamine dendrimer. *J. Biosci. Bioeng.* **95**(5):541–543 (2003).
171. M. J. Cloninger. Biological applications of dendrimers. *Curr. Opin. Chem. Biol.* **6**:742–748 (2002).
172. R. Esfand and D. A. Tomalia. Poly(amidoamine) (PAMAM) dendrimers: from biomimicry to drug delivery and biomedical applications. *DDT* **6**(8):427–436 (2001).
173. J. F. G. A. Jansen, E. M. M. De Brabander-van den berg, and E. W. Meijer. Encapsulation of guest molecules into a dendritic box. *Science* **266**:1226–1229 (1994).
174. D. Bhadra, A. K. Yadav, S. Bhadra, and N. K. Jain. Glycodendrimeric nanoparticulate carriers of primaquine phosphate for liver targeting. *Int. J. Pharm.* **295**:221–223 (2005).
175. R. X. Zhou, B. Du, and Z. R. Lu. *In vitro* release of 5-fluorouracil with cyclic core dendritic polymer. *J. Control. Release* **57**(3):249–257 (1999).
176. M. El-Sayed, M. F. Kiani, M. D. Naimark, A. H. Hikal, and H. Ghandehari. Extravasation of poly(amidoamine) (PAMAM) dendrimers across microvascular network endothelium. *Pharm. Res.* **18**:23–28 (2001).
177. F. Tajarobi, M. El-Sayed, B. D. Rege, J. E. Polli, and H. Ghandehari. Transport of poly amidoamine dendrimers across Madin–Darby canine kidney cells. *Int. J. Pharm.* **215**:263–267 (2001).
178. R. F. Barth, D. M. Adams, A. H. Soloway, F. Alam, and M. V. Darby. Boronated starburst dendrimer-monoclonal antibody immunoconjugates: evaluation as a potential delivery system for neutron capture therapy. *Bioconjug. Chem.* **5**:58–66 (1994).
179. R. Wiwattanapatapee, B. Carrenño-Gómez, N. Malik, and R. Duncan. Anionic PAMAM dendrimers rapidly cross adult rat intestine *in vitro*: a potential oral delivery system? *Pharm. Res.* **17**:991–998 (2000).
180. A. K. Patri, I. J. Majoros, and J. R. Baker Jr. Dendritic polymer macromolecular carriers for drug delivery. *Curr. Opin. Chem. Biol.* **6**:466–471 (2002).
181. N. Malik, R. Wiwattanapatapee, R. Klopsch, K. Lorenz, H. Frey, J. W. Weener, E. W. Meijer, W. Paulus, and R. Duncan. Dendrimers: relationship between structure and biocompatibility *in vitro*, and preliminary studies on the biodistribution of 125I-labelled polyamidoamine dendrimers *in vivo*. *J. Control. Release* **65**:133–148 (2000).
182. T. M. Chapman, G. L. Hillyer, E. J. Mahan, and K. A. Shaffer. Hydraamphiphiles: novel linear dendritic block copolymer surfactants. *J. Am. Chem. Soc.* **116**:11195–11196 (1994).
183. X. F. Zhong and A. Eisenberg. Aggregation and critical micellization behavior of carboxylate-terminated monochelic polystyrene. *Macromolecules* **27**(7):1751–1758 (1994).
184. J. C. M. Van Hest, D. A. P. Delnoye, M. W. P. L. Baars, M. H. P. van Genderen, and E. W. Meijer. Polystyrene-dendrimer amphiphilic block copolymer with a generation-dependent aggregation. *Science* **268**:1592–1595 (1995).
185. L. Y. Zhu, G. L. Zhu, M. Z. Li, E. J. Wang, R. P. Zhu, and X. Qi. Thermosensitive aggregates self-assembled by an asymmetric block copolymer of dendritic polyether and poly (*n*-isopropylacrylamide). *Eur. Polym. J.* **38**(12):2503–2506 (2002).
186. M. Schappacher, J. L. Putaux, C. Lefebvre, and A. Deffieux. Molecular containers based on amphiphilic PS–*b*-PMVE dendrigraft copolymers: topology, organization, and aqueous solution properties. *J. Am. Chem. Soc.* **127**:2990–2998 (2005).